Insurance: Mathematics and Economics 64 (2015) 364–379

Contents lists available at ScienceDirect

Insurance: Mathematics and Economics

journal homepage: www.elsevier.com/locate/ime

Pricing guaranteed minimum/lifetime withdrawal benefits with various provisions under investment, interest rate and mortality risks

Tian-Shyr Dai [a], Sharon S. Yang [b,c,*], Liang-Chih Liu [a]

[a] Department of Information and Financial Management and Institute of Finance, National Chiao-Tung University, Taiwan

[b] Department of Finance, National Central University, Taiwan

[c] Risk and Insurance Research Center, College of Commerce, National Chengchi University, Taiwan

ARTICLE INFO

Article history:
Received March 2014
Received in revised form
March 2015
Accepted 7 April 2015
Available online 27 April 2015

Keywords:
Guaranteed life withdrawal benefits
Surrender option
Variable annuity
Interest rate risk
Mortality risk

ABSTRACT

Many variable annuity products associated with guaranteed minimum withdrawal benefit (GMWB) or its lifelong version, a guaranteed lifelong withdrawal benefit (GLWB), have enjoyed great market success in the United States and Asia. The interaction impacts among complex policy provisions and the randomness of the account value of the policy, the prevailing interest rate, as well as the mortality rate may significantly influence the evaluations of GMWBs/GMLBs, especially when the guaranteed payments are made over a long, or even a lifelong, horizon. To deal with aforementioned risk factors and policy provisions, this paper proposes a novel three-dimensional (3D) tree that can analyze how different policy provisions influence the evaluation of GMWB/GLWBs under investment interest rate, and mortality risks simultaneously. The orthogonalization method is used to convert correlated dynamics of the account value of the policy and the short-term interest rate into two independent processes that can be easily simulated by our 3D tree. Besides, the structure of our 3D tree is sophisticatedly designed to avoid the unstable (oscillating) pricing results phenomenon that has characterized many numerical pricing methods. Rigorous numerical experiments are given to analyze the interaction effects among policy provisions and the aforementioned risk factors on the evaluation of GMWBs/GLWBs.

1. Introduction

The variable annuity (VA) is a popular insurance product sold in insurance markets. Differing from a traditional life insurance product, a VA product allows the policyholder to choose the investment portfolio and thus bear the profit or loss due to the investment performance. To protect the policyholder from the downside investment risk, granting an investment guarantee has become a popular rider attached to VA products. With this design, the policyholder is guaranteed to receive a prespecified stream of return(s) from the issuer through various types of investment guarantees, such as guaranteed minimum death benefits (GMDBs), guaranteed minimum maturity benefits (GMMBs), guaranteed minimum income benefits (GMIBs), and guaranteed minimum withdrawal benefits (GMWBs). For simplicity, the aforementioned policies are collectively referred to as "GMXBs". These VA products have enjoyed great market success both in the United States and Asia.

The GMWB rider recently introduced by Hartford in 2002 has become a popular innovated design for VAs (see Yang and Dai, 2013). A GMWB rider protects the policyholder against the downside investment risk by providing him/her with the right to regularly withdraw a fixed rate[1] of a contractually specified amount from the investment account over a prespecified withdrawal period. Recently, this guaranteed withdrawal period of a GMWB rider has been extended to be lifelong, to which we refer by guaranteed lifetime withdrawal benefits (GLWBs hereafter). For a GLWB rider, the withdrawal rate may depend on the issue age[2] and there is no limit for the total amount that is withdrawn over the term of the policy. The remaining investment will be returned to the policyholder (or the insured's beneficiary) when a GMWB expires (or a GLWB holder dies). A GLWB rider has become very

* Corresponding author at: Department of Finance, National Central University, Taiwan.

E-mail addresses: cameldai@mail.nctu.edu.tw (T.-S. Dai), syang@ncu.edu.tw (S.S. Yang), tony919kimo@gmail.com (L.-C. Liu).

http://dx.doi.org/10.1016/j.insmatheco.2015.04.003
0167-6687/

[1] This rate is guaranteed to return at least the entire investment.

[2] It refers to the policyholder's age when the policy was first issued.

popular in the US market (see Otar, 2007; LIMRA, 2013). According to a report by LIMRA in 2013, the election rates of GLWB, GMWB, GMIB, and GMAB are 81%, 2%, 15%, and 2%, respectively.

The granting of GMXBs can be treated as exotic options embedded in VA products. Evaluating these VA products and embedded exotic options is critical for an insurance company to determine the hedging strategies and the fair charge—a fair amount of the insurance fee that makes the policy value (or the present value of future cash flows received from the policy) equal to the present value of investments. Evaluating a GMWB has drawn much attention in the academic literature in recent years since this policy is popular and has many complex provisions. Milevsky and Salisbury (2006) price GMWBs by taking advantage of the concept of a Quanto Asian put. Chen et al. (2008) then consider the jump risk in the account value and employ a jump–diffusion process to evaluate the GMWBs. Dai et al. (2008) instead provide a rigorous derivation of the singular stochastic control model for pricing variable annuities with GMWB using the Hamilton–Jacobi–Bellman (HJB) equation. Bauer et al. (2008) consider a universal pricing framework for pricing various GMXBs by using simulation techniques. Yang and Dai (2013) analyze the impacts of different provisions on the pricing of the GMWBs.

The aforementioned pricing models are based on a constant interest rate environment. However, ignoring the interest rate risk would significantly misprice a policy, since interest-rate-sensitive instruments are usually important components of the corresponding investment portfolio. This price deviation problem becomes significant with the increment of the policy's maturity, especially for a lifelong policy such as a GLWB. Recently, a few studies have examined the GLWB rider (see Piscopo and Haberman, 2011; Holz et al., 2012), but they have not considered the interest rate risk. The interest rate risk seems to have been first considered by Nielsen and Sandmann (1995) to price an equity-linked life insurance. Lin and Tan (2003) and Kijima and Wong (2007) further consider the pricing of equity-indexed annuities and show that the interest rate risk becomes significant when valuing long-duration insurance policies. Peng et al. (2012) first analyze the interest rate risk for pricing GMWBs by employing the Vasicek model (see Vasicek, 1977) that cannot exactly fit the real market zero rate curves. Due to the mathematical complexity, they derive lower and upper bounds for the GMWB value without considering various provisions of GMWBs. Our paper goes further to price GMWBs/GLWBs under the extended Vasicek model (see Hull and White, 1994), which can exactly fit the prevailing zero curve.

In addition, the longevity risk plays a significant role in pricing GMWBs/GLWBs (see Piscopo and Haberman, 2011; Yang and Dai, 2013; Fung et al., 2013), especially for the later one. Piscopo and Haberman (2011) and Fung et al. (2013) point out that the issuers of lifetime-payment guarantees may suffer from longevity risk since policyholders on average live longer than expected. Yang and Dai (2013) adopt a deterministic mortality model in pricing the GMWB contracts and did not address the issue of longevity risk. This study further examines the GLWB contracts and considers the critical issue of longevity risk for such contracts. Biffis (2005) propose an affine jump–diffusion mortality process that can provide a flexible framework for actuarial valuations of a number of life insurance contracts. Thus, we further incorporate the stochastic mortality model proposed by Biffis (2005) into our pricing model for both GMWB and GWLB contracts and reflect its impacts associated with different product features.

Yang and Dai (2013) argue that many popular provisions as well as the surrender option embedded in GMWBs significantly influence the evaluations of fair charges. A GMWB/GLWB policy may grant a policyholder the right to surrender the policy to redeem the whole account value or to over-withdraw from the account subject to a predetermined early redemption penalty. A policyholder will surrender the policy (or over-withdraw from the account) if he or she finds that the value of redeeming early exceeds the value of the withdrawal guarantee minus the losses of the insurance fee, the mortality risk, and the time value due to postponed withdrawals. Ignoring the surrender option provision may result in strong price deviations for different types of GMXB as mentioned in Shen and Xu (2005), Costabile et al. (2008), and Yang and Dai (2013). Similarly, many studies (see Chen et al., 2008; Dai et al. (2008)) have carefully studied the partial withdrawal provision; that is, the policyholder is allowed to withdraw any amount from the account to maximize his/her benefit.

However, the values of such provisions and the surrender option could be affected not only by the future investment uncertainty but also the interest rate and mortality rate risks. To make a valuation framework for GMWB/GLWBs more realistically, we extend Yang and Dai (2013) by analyzing all provisions mentioned in their paper under a stochastic investment, interest rate and mortality rate environment simultaneously. In other words, we focus on how the presence of the investment risk, the interest rate risk, the mortality risk, and other provisions influence the surrender option premium. Our work can also analyze the optimal withdrawal behaviors by mimicking the method in Yang and Dai (2013). Extending, we further considers another two popular provisions: a ratchet guarantee provision and a regular premium provision. In most GMWBs/GLWBs, policyholders are required to invest their policy accounts during the so-called "deferral period" and the guaranteed withdrawals are deferred to take place at the beginning of the so-called "withdrawal period". A ratchet guarantee determines the amount of total guaranteed withdrawals as the maximum of the policy account value during the deferral period. A regular premium provision requires a policyholder to invest the account periodically during the deferral period. While our numerical experiments suggest that these two provisions would significantly influence the evaluation of GMWBs/GLWBs, most existing works may significantly misprice the policies due to the ignorance of the deferral period and the provisions.

Our paper constructs a three-dimensional (3D) tree to simultaneously model the investment, the interest rate, and the mortality risks for pricing GMWBs/GLWBs. Compared to a univariate pricing method (like the Yang and Dai, 2013 method that only models the dynamics of the account value), developing a multivariate method elevates the difficulty to a new level due to the following problems. First, directly modeling the aforementioned risks simultaneously will result in the "curse of dimensionality"; that is, we need to build a high-dimension tree[3] that makes the tree structure too complex to deal with. Second, it is hard to build a feasible tree to match the correlations among correlated processes being simulated (see Zvan et al., 2003). Third, it is also hard to build a tree to simultaneously match the moments of several processes with stochastic drift terms as mentioned in Lyuu and Wang (2011). Finally, many numerical methods generate oscillating pricing results due to the nonlinearity error as mentioned in Figlewski and Gao (1999), and this undesirable property may make the evaluation of the fair charge intractable. Recall that the fair charge denotes a fair amount of the insurance fee that makes the policy's value equal to the present value of investments. Oscillating pricing results for the policy's value would make the above equilibrium unsolvable. The oscillating pricing problem can be alleviated by making some tree nodes coincide with the "critical locations"—the locations where the function of the policy's value is highly nonlinear as suggested in Dai and Lyuu (2010).

[3] In this case, we require four dimensions for time, the account value, the short rate, and the mortality risk.

Our 3D tree is sophisticatedly designed to address the above problems. First, by adopting the assumption that the mortality risk is independent of the investment and the interest rate risks,[4] we will prove in a later section that the curse of dimensionality can be alleviated. Thus we can first build our 3D tree to simulate the dynamics of the account value and the short rate. The mortality risk can be taken into account by first evaluating the expected mortality rate at each time step (of our 3D tree) and then by incorporating these expected mortality rates into our tree. Reducing tree dimension from four to three not only avoid complex tree construction procedure but also significantly reduce the computational time required to evaluate a GMWB/GLWB policy. To address the second problem, we first convert the account value and the short rate processes into two uncorrelated processes by means of the orthogonalization method. Then our tree models the evolution of these two uncorrelated processes to avoid invalid tree structures due to the correlation calibration. To address the last two problems, we take advantage of the "mean-tracking" tree construction method proposed by Dai (2009) to adjust our 3D tree. The tree structure is adjusted to match the drift term of the account value or to make some tree nodes coincide with critical locations to alleviate the oscillating pricing problem. Our numerical experiments show that our robust 3D tree can reasonably analyze the interaction effects among investment risk, interest rate risk, mortality risk, and various provisions that are not well studied in the previous literature.

The remainder of this paper is organized as follows. In Section 2, we describe a GMWB/GLWB policy and its various provisions, and then express the underlying mathematical models used to model the investment risk, the interest rate risk, and the mortality risk. In Section 3, we construct a 3D tree to model the aforementioned three risks and discuss how we adjust the tree structure to avoid infeasible tree structures and oscillating pricing results. In Section 4, we analyze the impacts of the aforementioned risks and various provisions of GMWBs/GLWBs on their values and fair charges. Section 5 concludes the paper.

2. Financial settings and mathematical models

2.1. Introduction to GMWBs/GLWBs

The life span of a GMWB policy can be divided into the deferral period with length T_1 and the withdrawal period with length T_2. A policyholder is allowed to either invest the policy account once at the inception of the deferral period (i.e., a single premium) or to invest the account periodically during the deferral period (i.e., regular premium). In return for the investment, the policyholder can periodically withdraw a specified amount from the account during the withdrawal period. Let $W(t)$ denote the account value at time t. During the deferral period (from time 0 to time T_1), the account value $W(t)$ jumps up with the investment amount I at an investment date and otherwise follows a lognormal diffusion process due to the change in the value of the investment and the payment of the fair charge. Thus, under a regular premium setting, the process of $W(t)$ at an investment date τ follows

$$W(\tau^+) = W(\tau^-) + I, \tag{1}$$

where τ^- and τ^+ denote the times immediately before and after time τ, respectively. Under a single premium setting, we set $W(0^+) = I$. Between any two investment dates, the dynamics of $W(t)$ follows

$$dW(t) = (r(t) - \alpha)\, W(t)dt + \sigma W(t)dB(t), \tag{2}$$

where $r(t)$ denotes the prevailing short rate (introduced later), σ represents the volatility of the account value process, and $B(t)$ denotes the Brownian motion. The fair charge α refers to a proper rate received by the insurance company that makes a GMWB value – the present value of expected future cash flows received from the GMWB – equal to the present value of the policyholder's investment.

On the other hand, the holder is allowed to periodically withdraw the guaranteed withdrawal amount G from the GMWB account at each withdrawal date during the withdrawal period (from time T_1 to the maturity date $T_1 + T_2$). If the account value is insufficient to finance the withdrawal, the policyholder is guaranteed to receive G and the account value becomes 0. The fall in the account value due to a discrete withdrawal at a withdrawal date τ can be expressed as

$$W(\tau^+) = \max(W(\tau^-) - G, 0). \tag{3}$$

Between any two withdrawal dates, $W(t)$ follows the lognormal diffusion process as in Eq. (2).

A GLWB policy is similar to a GMWB one except that the former policy does not have an explicit maturity; that is, it will not terminate unless the policyholder surrenders the policy early or the policyholder dies. Since human mortality experiences in many countries show that 110 is the maximum survival age, we incorporate this age-limit finding into our numerical analysis. Thus our finite-time-spanned numerical method can easily adopt these mortality models to evaluate a GLWB by setting the length of the withdrawal period T_2 as the maximum survival age minus T_1 and the issue age.

Next, let us review various provisions embedded in GMWBs/GLWBs. The lump sum of guaranteed withdrawal amounts is usually set as the maximum of a contract-specified value $C(T_1)$ and the account value at the end of the deferral period $W(T_1)$. $C(T_1)$ can be determined by a principal guarantee or a rollup interest rate guarantee (see Yang and Dai, 2013). This paper will further analyze the impact of a ratchet guarantee; that is, $C(T_1)$ is defined as the maximum of the account value during the deferral period. The guaranteed withdrawal amount G at each withdrawal date can be expressed as

$$G = \frac{\mathrm{Max}[C(T_1), W(T_1)]}{\lambda T_2} = \frac{g\mathrm{Max}[C(T_1), W(T_1)]}{\lambda}, \tag{4}$$

where λ denotes the number of withdrawal dates per year, and g denotes the proportion of the value that will be withdrawn per year. In a GMWB policy, the length of the withdrawal period T_2 is given and g is set to $1/T_2$. On the other hand, a GLWB policy provides a lifelong guarantee without determining T_2 and thus g is exogenously specified in the policy.

The aforementioned model of account dynamics presents a general structure of a deferred variable annuity embedded in GMWBs/GLWBs. Most research papers (e.g., Milevsky and Salisbury, 2006; Dai et al., 2008; Chen et al., 2008, and so on) ignore the deferral period and their setting is a degenerated case of our model by setting $T_1 = 0$ and $C(T_1) = W(0)$. Yang and Dai (2013) argue that ignoring the deferral period and corresponding provisions might significantly misprice the policies. This paper extends their work by analyzing all provisions mentioned in their paper plus two other ones: a regular premium and a ratchet guarantee, under the stochastic interest rate and the mortality rate environment.

Surrender options are embedded in most GMWBs/GLWBs to allow policyholders to surrender their policies prior to maturity. A rational policyholder will surrender the policy early once he or she finds that the continuation value of the policy is less than the early redemption value. The continuation value is the value to hold the policy without surrendering the policy immediately, and this

[4] Piscopo and Haberman (2011), Holz et al. (2012) and Yang and Dai (2013) also assume that the mortality rate is independent of the investment risk.

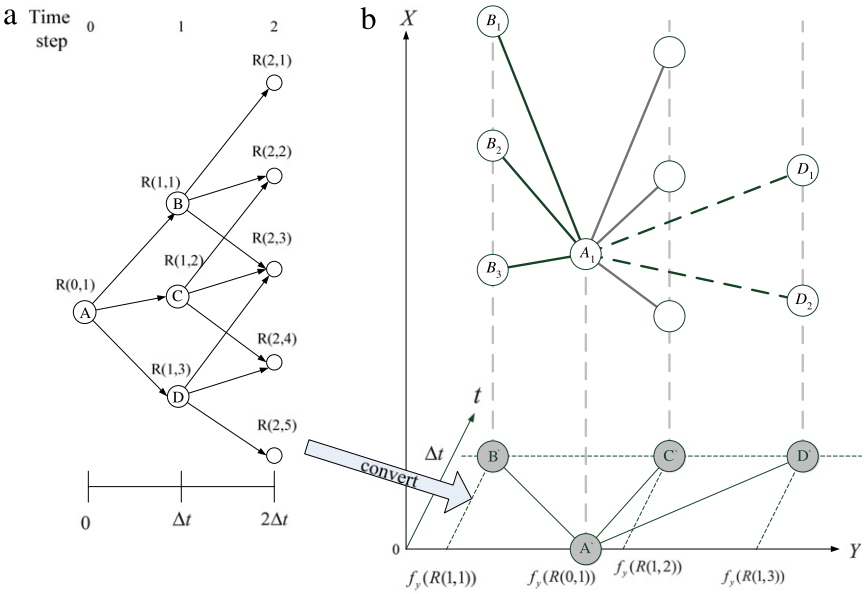

Fig. 1. A brief illustration for converting the Hull–White interest rate tree to the foundation of our 3D Tree. Notes: Panel (a) shows the brief structure for the Hull–White interest rate tree. $R(0, 1)$, $R(1, 1)$, $R(1, 2)$, and $R(1, 3)$ denote the short rates for nodes **A**, **B**, **C**, and **D**, respectively. Panel (b) presents a brief structure of our 3D tree (formed by the hollow nodes) and the converted interest rate tree (formed by the gray nodes). The pillars of $R(0, 1), \ldots, R(1, 3)$ are marked by the gray dashed lines.

value can be evaluated as the present value of future expected cash flows generated from holding the policy. On the other hand, surrendering the policy allows a policyholder to over-redeem the remaining account value subject to an early redemption penalty; thus, the early redemption value at a withdrawal date t is

$$G + (1 - k)(W_t - G),$$

where k denotes the proportional penalty charge. Obviously, a rational policyholder will surrender the policy if the loss of the time value due to postponing withdrawals plus the future mortality risk and the interest rate risk exceeds the early redemption penalty $k(W_t - G)$. The complex relationships among the surrender option premium, other provisions, interest rate risk, and mortality risk will be studied in this paper.

A partial withdrawal provision allows a policyholder to withdraw any amount from the account to maximize his or her benefit. Yang and Dai (2013) show that their tree can model this provision by using more state variables to keep the information required to analyze different withdrawal strategies as proposed in Hull and White (1993). Their method can be easily incorporated into our 3D tree model. While the partial withdrawal provision has been widely studied in much of the literature (see Chen et al., 2008; Dai et al., 2008), the relationships among the surrender options, other provisions, and market variables are rarely studied (see Yang and Dai, 2013). Thus this paper will focus on the analyses of surrender options.

2.2. Review of mathematical and numerical models

The mathematical and numerical models adopted to construct our 3D tree to analyze the impact of the market price risk, the interest rate risk, and the mortality risk are sketched separately as follows.

The interest rate dynamics

The Hull–White interest rate model (see Hull and White, 1990) is a no-arbitrage short rate model that can calibrate the prevailing zero rate curve. The short rate at time t, $r(t)$, follows the stochastic process

$$dr(t) = a(\theta(t) - r(t))dt + \eta dZ_2(t), \tag{5}$$

where a is the mean-reverting rate, $\theta(t)$ is a function of time to calibrate the prevailing zero rate curve, η is the interest rate volatility, and $Z_2(t)$ denotes a Brownian motion. The aforementioned interest rate dynamics can be discretely simulated by a trinomial interest rate tree proposed by Hull and White (1994) as illustrated in Fig. 1(a). A tree divides a certain time interval $[0, T]$ into n time steps, each with length Δt ($\equiv T/n$). It discretely specifies the values and the evolutions for simulated variable(s) at each time step. For example, the short rate $R(0, 1)$ at time step 0 will move to $R(1, 1)$, $R(1, 2)$, or $R(1, 3)$ at time step 1, where $R(i, j)$ denotes the short rate for the jth node at the ith time step.

It is hard to build a feasible tree for modeling correlated processes as mentioned in Zvan et al. (2003). Thus, we convert the account value process and the short rate process into two independent processes $X(t)$ and $Y(t)$[5] by the orthogonalization method discussed in the next section. Then we build a 3D tree to model the evolution of $X(t)$ and $Y(t)$ as illustrated in Fig. 1(b). We will show that $Y(t)$ can be expressed as a linear function f_y of the short rate, and thus the Hull–White interest rate tree in Fig. 1(a) can be converted to construct the foundation of our 3D tree (or the "converted interest rate tree" formed by gray nodes in Fig. 1(b)). Our 3D tree is built based on the converted interest rate tree to model the evolution of $X(t)$, which governs part of the account value dynamics that is uncorrelated with the short rate.

The account value dynamics

To model the properties of the account value process, a log-normal diffusion process (see Eq. (2)) with periodical jumps due to investments and withdrawals (see Eqs. (1) and (3)), $X(t)$, will follow the drift-varying diffusion process $dX(t) = m_x(t, r(t))dt + dZ(t)$[6] with periodical jumps. The diffusion process can be simulated by the CRR tree (see Cox et al., 1979), and the jumps in $X(t)$ can be modeled by the stair tree (see Dai, 2009). Besides, to avoid oscillating pricing results caused by various provisions of GMWBs/GLWBs, we adopt the core idea of the bino-trinomial tree

[5] See Section 3.1 for the detailed definitions of $X(t)$ and $Y(t)$.

[6] The drift term $m_x(t, r(t))$ will be derived in the next section, and $dZ(t)$ denotes a Brownian motion.

(see Dai and Lyuu, 2010). Although the three aforementioned tree models are originally constructed based on a constant drift rate environment, we slightly modify their models so that they can be applied under a varying drift rate environment to construct our 3D tree.

A brief sketch of these tree models is illustrated in Fig. 2. A discrete-time tree can properly simulate $X(t)$ by adjusting the movements and the branching probabilities to make the first two moments implied by the tree structure match the moments of $X(t)$ (see Duffie, 1996). Take the CRR binomial structure beginning from node **A** (with value X_A at time τ) as an example. It may either move upward to node **B** (with value $X_B = X_A + \sqrt{\Delta t}$) with probability p or downward to node **D** (with value $X_D = X_A - \sqrt{\Delta t}$) with probability $1 - p$, where $p = \frac{e^{m_X(\tau, r(\tau))\Delta t + 0.5\Delta t^2} - e^{-\sqrt{\Delta t}}}{e^{\sqrt{\Delta t}} - e^{-\sqrt{\Delta t}}}$ to match the first two moments of the account value process.

Periodically, investments and withdrawals will lead to jumps in the account value process and hence jumps in $X(t)$ as illustrated by nodes **B** and **C** in Fig. 2. These jumps not only ruin the CRR tree structure, but also make the tree size and hence the computational time grow dramatically with the number of jumps. To avoid the so-called "combinatorial explosion" problem, the stair tree proposed by Dai (2009) suggests that a trinomial structure can be inserted to connect an after-jump node like node **C** back to the nodes that follow the CRR tree structure at time $\tau + 2\Delta t$. He proposes a mean-tracking method to ensure that the trinomial branch can be feasibly constructed to match the first two moments of $X(t)$. Specifically, the outgoing middle branch from node **C** will connect to node **F**, whose value is closest to $X_c + m_x(\tau + \Delta t, r(\tau + \Delta t))$, the conditional expected value of $X(\tau + 2\Delta t)$ given that $X(\tau + \Delta t) = X_c$. The other two branches will connect to the adjacent nodes of node **F**. The trinomial branch probabilities are then solved by matching the first two moments of $X(t)$ as follows[7]:

$$\begin{cases} p_u = (\beta\gamma + \Delta t)(\gamma - \beta)/\phi \\ p_m = (\delta\gamma + \Delta t)(\delta - \gamma)/\phi \\ p_d = (\delta\beta + \Delta t)(\delta - \beta)/\phi, \end{cases} \tag{6}$$

where $\phi = (\beta - \delta)(\gamma - \beta)(\gamma - \delta)$, δ, β, and γ denote the values of nodes **E**, **F**, and **H** minus the conditional expected value $X_c + m_x(\tau + \Delta t, r(\tau + \Delta t))$.

The nonlinearity error (discussed in Figlewski and Gao, 1999) may cause a policy value evaluated by a tree to oscillate significantly as illustrated by the thin gray curve plotted in Fig. 3(a). This oscillation prevents us from stably finding the fair charge, a proper insurance rate that makes the policy value equal the present value of a policyholder's investment (denoted by the black dashed line). Specifically, multiple solutions will be found since the oscillating thin gray curve crosses the black dashed line at multiple points, like α_1, α_2, and α_3. To stably measure the fair charge α without the disturbance of the nonlinearity error problem, the structure of our 3D tree is sophisticatedly designed to generate smoothed pricing results as plotted by the solid black curve in Fig. 3(a). We follow Dai and Lyuu (2010)'s core idea by making some tree nodes coincide with the so-called "critical locations", that is, the places where the policy value function is highly nonlinear due to kinks. Two types of kinks can be identified in a GMWB/GLWB policy. The first type occurs at time T_1 when the account value equals $C(T_1)$ as illustrated in Fig. 3(b). This is because the lump sum of the guaranteed withdrawal amounts is set to the maximum of $C(T_1)$ and $W(T_1)$ (see Eq. (4)). The second type occurs at each withdrawal date when the account value equals the guaranteed withdrawal amount G. This is because the guaranteed withdrawal provision allows the policyholder to withdraw G from the account even if the account value is insufficient. Finally, Fig. 2 sketches how we make a node, say, **I**, match a critical location. Let time $\tau + 2\Delta t$ be a withdrawal date. The value for node **I**, Ω, is properly selected to make the corresponding account value at node **I** be G.[8] The values for other nodes at time $\tau + 2\Delta t$ are designed to have the forms $\ldots, \Omega + 2k\sqrt{\Delta t}, \Omega + (2k+2), \ldots$, where k denotes an integer; that is, the nodes at time $\tau + 2\Delta t$ still follow the layout of the CRR tree to avoid the aforementioned combinatorial explosion problem.

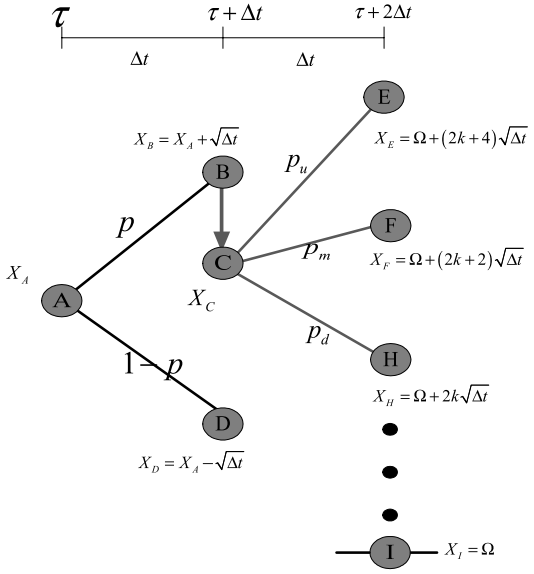

Fig. 2. A brief sketch of the CRR tree, the stair tree, and the BTT. Notes: The evolution of $X(t)$ during the time interval $[\tau, \tau + \Delta t]$ is modeled by the CRR tree. The down jump from node **B** to node **C** reflects the jump in the account value and the outgoing trinomial structure is constructed by taking advantage of the stair tree. The layout of nodes at time $\tau + 2\Delta t$ follows the layout of the CRR tree. To alleviate the oscillating pricing problem by taking advantage of the core idea of BTT, node **I** is designed to coincide with the critical location marked by the thick black line. The value for each node is listed next to the node. The branching probability like p and p_u for each branch is directly marked on that branch. The variable k denotes an integer.

The mortality dynamics

When a policyholder dies, the withdrawal guarantees of the GMWB/GLWB are annulled and the remaining account value is returned to the beneficiary. Due to the longevity risk and the occasional spread of high-lethal-rate diseases, ignoring mortality uncertainty will significantly misprice a long-term policy like a GMWB/GLWB. Although developing a robust mortality model is not the focus of our research, we provide a flexible pricing approach that can adopt a wide class of mortality models. In this paper, we first sketch a special case (Vasicek, 1977 model) of Biffis (2005)'s affine stochastic mortality model in this Section and then demonstrate how his model is incorporated into our 3D tree in the next section. Biffis (2005) decomposes the mortality rate μ_t^x into a deterministic function of time and age $u_x(t)$ plus a mean reverting stochastic process Y_t^D, which represent the current estimation of the future mortality rate and the uncertainty of the future mortality rate, respectively. His model can be expressed as follows:

$$\begin{aligned} \mu_t^x &= u_x(t) + Y_t^D \\ dY_t^D &= a_D\left(b_D - Y_t^D\right)dt + \sigma_D dZ_t, \end{aligned} \tag{7}$$

where μ_t^x denotes the tth-year mortality rate of a person whose age is x in year 0, $u_x(t)$ denotes the estimation of μ_t^x, Y_t^D follows

[7] Dai (2009) shows that the above approach can generate a feasible trinomial structure without introducing negative branch probabilities.

[8] The detailed derivation of Ω will be discussed in Section 3.

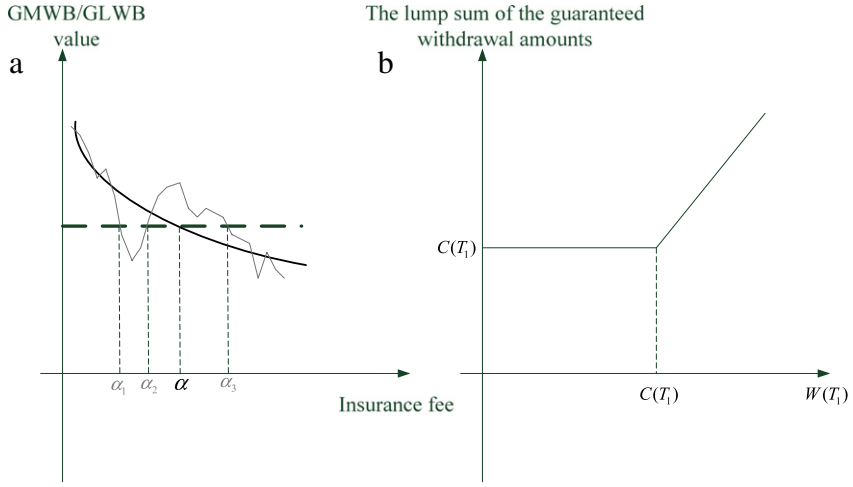

Fig. 3. Price oscillations and the nonlinearity error. Notes: Panel (a) plots the oscillating pricing results (the thin gray curve) and the smoothing pricing results (the solid black curve) generated by a naïve tree and our 3D tree, respectively. The black dashed line denotes the present value of the policyholder's investment. Panel (b) points out the kink of the GMWB/GLWB value functions at time T_1.

a mean reverting process with the long-term average level b_D, the mean reverting speed a_D, and the volatility σ_D.

To obtain the fair value of GMWB/GLWB contracts, we follow Biffis (2005) using a risk-neutral adjustment to the mortality rate on the same realistic basis.[9] Thus, the risk-neutral probability for a person aged $x+\tau$ to survive for $s-\tau$-years, denoted as ${}_{s-\tau}p_{x+\tau}$, is evaluated as

$$\begin{aligned} {}_{s-\tau}p_{x+\tau} &= E^Q\left[e^{\left(-\int_\tau^s \mu_u^x du\right)}|g_\tau\right] \\ &= \underbrace{e^{\left(-\int_\tau^s \mu_x(u)du\right)}}_{{}_{s-\tau}\bar{p}_{x+\tau}} \underbrace{E^Q\left[e^{-\int_\tau^s Y_u^D du}|g_\tau\right]}_{\mathrm{ADJ}^Q(\tau,s,Y_\tau^D)}, \end{aligned} \tag{8}$$

where the sequence $(g_t)_{t\in R^+}$ denotes the filtration, and the σ-algebra g_t can be interpreted as the information available up to time t. The risk-neutral survival rate can be decomposed into two components: the constant component ${}_{s-\tau}\bar{p}_{x+\tau}$ can be evaluated by directly integrating the function $u_x(t)$ over the time interval $[\tau, s]$, and the risk-neutral adjustment component $\mathrm{ADJ}^Q(\tau, s, Y_\tau^D)$ can be evaluated by taking advantage of the bond pricing formula of the Vasicek (1977) interest rate model. Specifically, the risk-neutral adjustment component can be expressed as

$$\begin{aligned} \mathrm{ADJ}^Q(\tau, s, Y_\tau^D) &:= E^Q\left[e^{-\int_\tau^s Y_u^D du}|g_\tau\right] \\ &= \exp(A(\tau,s) - B(\tau,s)Y_\tau^D), \end{aligned}$$

where $B(\tau,s) = \frac{1-e^{-a_D(s-\tau)}}{a_D}$, and $A(\tau,s) = \left(B(\tau,s) - (s-\tau)\right)\left(b_D - \frac{{\sigma_D}^2}{2{a_D}^2}\right) - \frac{{\sigma_D}^2}{4a_D}B(\tau,s)^2$.

3. A novel tree for evaluating a GMWB/GLWB policy

To accurately evaluate a GMWB/GLWB policy, we construct a 3D tree that can simultaneously model the account value process, the short rate process, the mortality risk, and other various provisions. First, the orthogonalization method is used to convert the aforementioned two correlated processes into another two uncorrelated ones. As a result, the proposed 3D tree can model the evolution of these two uncorrelated processes instead. In addition, to make the 3D tree generate stable pricing results, the 3D tree is designed to coincide with the critical locations to alleviate the price oscillation problem as illustrated in Fig. 3(a). By adopting the assumption that the mortality risk is independent of the investment and the interest rate risks, we can prove that the mortality risk can be priced by simply incorporating the expected mortality rates evaluated in Eq. (8) into the proposed 3D tree. Finally, we explain how the backward induction procedure is designed to deal with various provisions, like surrender options. The following discussions focus on a GMWB policy, and the extension to a GLWB policy is straightforward.

3.1. Constructing uncorrelated processes by the orthogonalization method

To avoid the difficulty of constructing a tree that directly simulates the correlated processes simultaneously, we first convert the account value and the short rate processes into two uncorrelated ones by the orthogonalization method and then build a tree for these two uncorrelated processes instead. Let ρ denote the correlation between the account value process (see Eq. (2)) and the short rate process (see Eq. (5)); that is, $dB(t)dZ_2(t) = \rho dt$. Thus, $dB(t)$ can be rephrased as follows:

$$dB(t) = \rho dZ_2(t) + \sqrt{1-\rho^2}dZ_1(t),$$

where $Z_1(t)$ denotes another Brownian motion independent of $Z_2(t)$. Then the account value process and the interest rate process can be expressed in terms of $Z_1(t)$ and $Z_2(t)$ as follows:

$$\begin{aligned} \begin{bmatrix} d\ln W(t) \\ dr(t) \end{bmatrix} &= \begin{bmatrix} (r(t)-\alpha) - \dfrac{\sigma^2}{2} \\ a\theta(t) - a\cdot r(t) \end{bmatrix} dt \\ &\quad + \begin{bmatrix} \sqrt{1-\rho^2}\sigma & \rho\sigma \\ 0 & \eta \end{bmatrix} \begin{bmatrix} dZ_1(t) \\ dZ_2(t) \end{bmatrix}. \end{aligned} \tag{9}$$

By multiplying the inverse of the matrix $\begin{bmatrix} \sqrt{1-\rho^2}\sigma & \rho\sigma \\ 0 & \eta \end{bmatrix}$ on both sides of the above equation, two uncorrelated processes $X(t)$ and

[9] Due to the insurance market is not complete, for fair valuation purposes, Biffis (2005) employs the sense of *Draft Statement of Principles* and *International Financial Reporting Standard No. 4.* published by International Accounting Standards Board in 2001 and 2004, respectively, to deal with market valuation of life insurance contracts. (Also see IASB, 2001, 2004.)

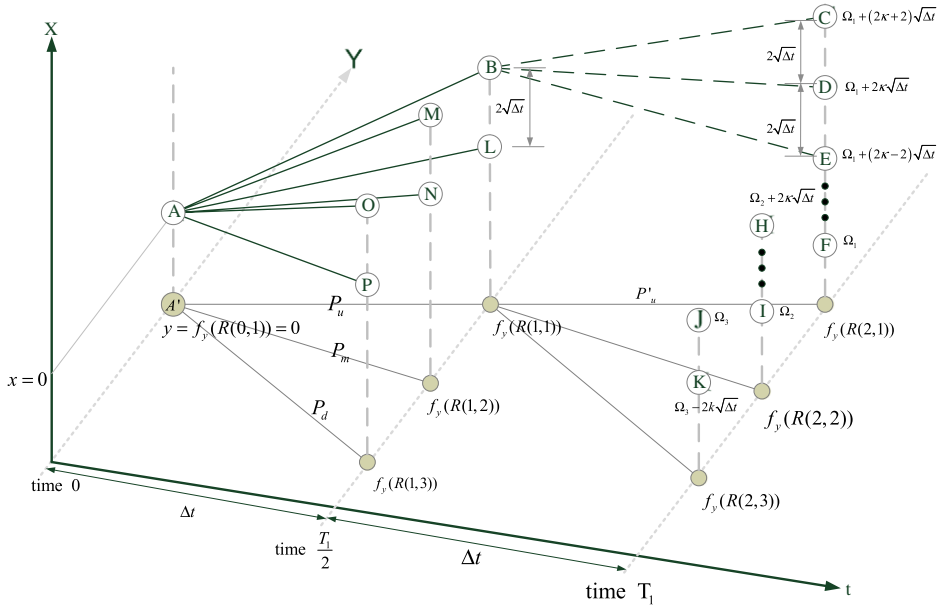

Fig. 4. A two-step deferral period tree. Notes: Δt denotes the length of a time step. The tree formed by gray-colored nodes on the Y–t plane denotes the converted interest rate tree discussed in Fig. 1(b). The Y coordinate for each node is listed next to the node. P_u, P_m, and P_d denote the outgoing branch probabilities from $\mathbf{A}'$ to the following nodes at time $T_1/2$. P'_u denotes the probability for moving from $f_y(R(1,1))$ to $f_y(R(2,1))$. Each pillar emitted by a gray color node is marked by a gray dashed line. The outgoing binomial branches emit from **A** to **B** and **L** at the pillar of $R(1,1)$, **M** and **N** at the pillar of $R(1,2)$, and **O** and **P** at the pillar of $R(1,3)$. The outgoing branches emitted from **L**, **M**, **N**, **O** and **P** are ignored for simplicity. The outgoing trinomial branches from **B** to **C**, **D**, and **E** at the pillar of $R(2,1)$ are plotted by black dashed lines. Other outgoing branches from node **B** are ignored for simplicity. The x coordinate for each node at time T_1 is listed next to the node. The account values for nodes **F**, **I**, and **J** are $C(T_1)$. The log-price-distance between two adjacent nodes at the same pillar is $2\sqrt{\Delta t}$.

$Y(t)$ are constructed as follows:

$$\begin{aligned}\begin{bmatrix} dX(t) \\ dY(t) \end{bmatrix} &\equiv \begin{bmatrix} \dfrac{d\ln W(t)}{\sigma\sqrt{1-\rho^2}} - \dfrac{\rho dr(t)}{\eta\sqrt{1-\rho^2}} \\ \dfrac{dr(t)}{\eta} \end{bmatrix} \\ &= \begin{bmatrix} \dfrac{(r(t)-\alpha)-\frac{\sigma^2}{2}}{\sigma\sqrt{1-\rho^2}} - \dfrac{\rho(a\theta(t)-ar(t))}{\eta\sqrt{1-\rho^2}} \\ \dfrac{(a\theta(t)-ar(t))}{\eta} \end{bmatrix} dt \\ &\quad + \begin{bmatrix} 1 & 0 \\ 0 & 1 \end{bmatrix} \begin{bmatrix} dZ(t) \\ dB_2(t) \end{bmatrix} \\ &\equiv \begin{bmatrix} m_x(t, r(t))dt + dZ(t) \\ m_y(t, r(t))dt + dB_2(t) \end{bmatrix}, \end{aligned} \tag{10}$$

where $m_x(t, r(t))$ and $m_y(t, r(t))$ denote the drift functions for $X(t)$ and $Y(t)$, respectively.

Now, by integrating both sides of Eq. (10) and by setting $X(0) \equiv Y(0) \equiv 0$. $X(t)$ and $Y(t)$ can interpreted as functions of $W(t)$ and $r(t)$ as follows:

$$\begin{cases} X(t) = \dfrac{1}{\sqrt{1-\rho^2}} \left[\dfrac{\ln \frac{W(t)}{W(0)}}{\sigma} - \rho \left(\dfrac{r(t)-r(0)}{\eta} \right) \right] \\ \quad \equiv f_x\left(W(t), r(t)\right) \\ Y(t) = \dfrac{r(t)-r(0)}{\eta} \equiv f_y\left((t)\right). \end{cases} \tag{11}$$

By solving the above equations, $W(t)$ and $r(t)$ can be interpreted as functions of $X(t)$ and $Y(t)$ as follows:

$$\begin{cases} W(t) = W(0) \exp\left(\sigma\left(\sqrt{1-\rho^2} \cdot X(t) + \rho \cdot [Y(t)]\right)\right) \\ r(t) = r(0) + \eta Y(t). \end{cases} \tag{12}$$

3.2. Constructing the 3D tree for the deferral and the withdrawal periods

We construct a 3D tree by simulating the evolution of $X(t)$ and $Y(t)$ introduced in Eqs. (9)–(11) during the deferral period and the withdrawal period. The corresponding account value and the short rate at each node in the tree can be obtained by substituting the $X(t)$ and the $Y(t)$ values of that node into Eq. (12). We first discuss how to convert the Hull–White interest rate tree into the foundation of our tree as illustrated in Fig. 1. Then we demonstrate the tree construction for the deferral period by using a two-time-step tree illustrated in Fig. 4. We call it the deferral-period tree for simplicity. Next, we demonstrate the tree construction for the withdrawal period by using another two-time-step tree illustrated in Fig. 5. We call it the withdrawal-period tree for simplicity. For brevity, the following discussion only focuses on the tree construction for modeling the account value drops due to periodical withdrawals. A similar method can be extended to model the upward jumps of the account value due to a regular premium provision.

Mapping the Hull–White interest rate tree into the foundation of our tree

We first map the short rate of each node in the Hull–White Tree as illustrated in Fig. 1(a) into its corresponding $Y(t)$ by the function f_y defined in Eq. (11) as illustrated in Fig. 1(b). For example, nodes **A** (with short rate $R(0,1)$), **B** (with short rate $R(1,1)$), and **D** (with short rate $R(1,3)$) map to node $\mathbf{A}'$ (with value $f_y(R(0,1))$), $\mathbf{B}'$ (with value $f_y(R(1,1))$), and $\mathbf{D}'$ (with value $f_y(R(1,3))$), respectively. In Fig. 1(b), the converted interest rate tree formed by gray nodes can be viewed as the foundation of our 3D tree composed of hollow nodes. Specifically, the projection of our 3D tree on the Y–t plane is the converted interest rate tree. For example, the y coordinates for both nodes $\mathbf{D_1}$ and $\mathbf{D_2}$ at time Δt are $f_y(R(1,3))$. These two nodes are passed through by the vertical gray dashed line emitted from node $\mathbf{D}'$; we call this line the pillar of $R(1,3)$ for simplicity. Similarly, nodes $\mathbf{B_1}$, $\mathbf{B_2}$, and $\mathbf{B_3}$

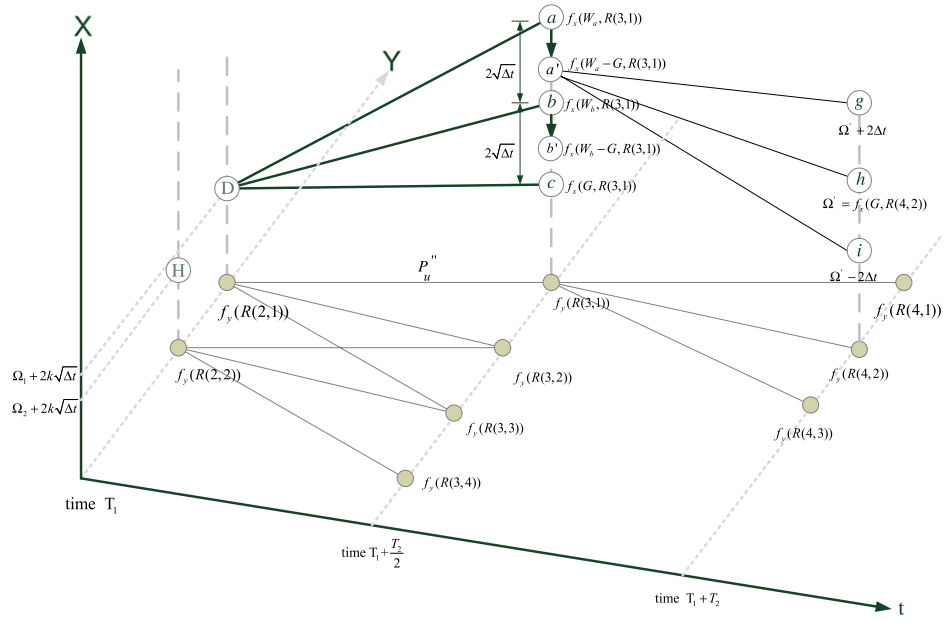

Fig. 5. A two-step withdrawal-period tree. Notes: The tree formed by gray-colored nodes on the Y–t plane denotes the converted interest rate tree discussed in Fig. 1(b). The tree begins from nodes **D** and **H** with coordinates $\left(\Omega_1 + 2k\sqrt{\Delta t}, f_y(R(2,1))\right)$ and $\left(\Omega_2 + 2k\sqrt{\Delta t}, f_y(R(2,2))\right)$, respectively. The policyholder is allowed to withdraw G from the account at time $(T_1 + T_2)/2$ and the corresponding downward jumps are reflected by the downward arrows. The x coordinates for the nodes at time $(T_1 + T_2)/2$ and $T_1 + T_2$ are listed next to the nodes. P_u'' denotes the branch probability moving from $f_y(R(2,1))$ to $f_y(R(3,1))$.

that are passed through by the pillar of $R(1,1)$ have the same y coordinate $f_y(R(1,1))$. Note that the outgoing branches from node $\mathbf{A_1}$ may either follow the trinomial branches (plotted in thick black solid lines) or the binomial branches (plotted in black dashed lines). The trinomial branches can be constructed by taking advantage of the mean-tracking method mentioned in Fig. 2, and are used to adjust the tree structure to connect after-jump nodes or to match critical locations. Otherwise, the CRR binomial branches are used to simplify our tree structure.

The deferral-period tree

The deferral-period tree in Fig. 4 begins at node **A** with coordinate $(0,0)$ since we set $X(0) = Y(0) = 0$ in Eq. (10). For an arbitrary node, say, **A**, the corresponding account value, say, $W(0)$, and the short rate, say, $r(0)$, can be obtained by substituting the coordinate of that node, say, $(0,0)$, into Eq. (12). We first focus on the converted interest rate tree (formed by gray nodes) constructed by converting the Hull–White interest rate tree as discussed in Fig. 1. From time 0 to time $T_1/2$, the process $Y(t)$ will move from $f_y(R(0,1))$ to $f_y(R(1,1))$, $f_y(R(1,2))$, and $f_y(R(1,3))$ with probabilities P_u, P_m, and P_d, respectively. The branch probabilities can be uniquely solved by matching the first two moments of process $Y(t)$ defined in Eq. (9). We then model the evolution of $X(t)$ based on the converted interest rate tree to form the 3D deferral-period tree. Two outgoing branches from node **A** will reach nodes **B** and **L** at the pillar of $R(1,1)$. This binomial structure follows the structure of the CRR tree introduced in Fig. 2 by setting the risk free rate $r(\tau)$ as $R(0,1)$. The x coordinates for node **B** and node **L** are $\sqrt{\Delta t}$ and $-\sqrt{\Delta t}$, respectively. Since $X(t)$ and $Y(t)$ are independent, the branch probability from node **A** to node **B** can be calculated as simply a direct multiplication of P_u by p, where p denotes the upward branch probability of the CRR tree defined in Fig. 2. Similarly, the branch probability from node **A** to node **L** is $P_u(1-p)$. The outgoing binomial branches from node **A** to **M** and **N** at the pillar of $R(1,2)$ and to **O** and **P** at the pillar of $R(1,3)$ are constructed in similar ways.

Recall that a kink in the policy value function occurs at time T_1 when the account value equals $C(T_1)$ as mentioned in Fig. 3(b). To alleviate the oscillation problem, we must have some nodes, say, **F**, **I**, and **J**, to match the kink. Specifically, the x coordinates for these three nodes, Ω_i $(i = 1, 2, 3)$, are equal to $f_x(C(T_1), R(2,i))$, where the function f_x is defined in Eq. (11). The nodes at the same pillar will follow the CRR tree structure, that is, the distance between two adjacent nodes at the same pillar is set as $2\sqrt{\Delta t}$. Thus, the x coordinate for each node at the pillar of $R(2,i)$ must have the form $\Omega_i + 2\ell\sqrt{\Delta t}$, where ℓ denotes an integer. Therefore, the outgoing branches emitted from the nodes at time T_1 can still follow the CRR binomial structure to avoid the aforementioned combinatorial explosion problem. To meet the change in the node structure at time T_1, the outgoing branches emitted from each node at time $T_1/2$ follow the trinomial structure constructed by the aforementioned mean tracking method. For example, node **B** will connect to node **D** and its two adjacent nodes **C** and **E** given that the x coordinate for node **D**. $\Omega_1 + 2k\sqrt{\Delta t}$ is closest to the conditional mean $X_B + m_x(T_1/2, R(1,1))\,\Delta t$ among the nodes at the same pillar, where X_B denotes the x coordinate of node **B**. The outgoing trinomial branch probabilities from node **B** can be obtained by substituting the x coordinates of nodes **C**, **D**, and **E** minus $X_B + m_x(T_1/2, R(1,1))\,\Delta t$ for δ, β, and γ into Eq. (6). Due to the independence of $X(t)$ and $Y(t)$, the branch probabilities from node **B** to nodes **C**, **D**, and **E** can be calculated as $P_u' p_u$, $P_u' p_m$, and $P_u' p_d$, respectively, where P_u' denotes the probability of moving from $f_y(R(1,1))$ to $f_y(R(2,1))$ in the converted interest rate tree. The outgoing branches from node **B** to the nodes located at the pillars of $R(2,2)$ and $R(2,3)$ and outgoing branches from other nodes at time $T_1/2$, say, **L**, to the nodes at time T_1 can also be constructed in the same way.

The withdrawal-period tree

Next, we discuss the construction of the withdrawal-period tree. For convenience, let W_z denote the account value at node $\boldsymbol{z}$. Several withdrawal-period trees are constructed to connect to the nodes of the deferral-period tree at time T_1, and each withdrawal-period tree begins from some nodes located at the end of the deferral period tree that determine the same guaranteed withdrawal amount G (see Eq. (4)).[10] Thus the sizes of the

[10] For simplicity, the following discussion only focuses on the principal guarantee and the rollup interest rate guarantee designs. To deal with the ratchet guarantee

downward jumps of the account value (marked by the downward arrows) in the same withdrawal-period tree must be identical. For example, the guaranteed withdrawal amount determined by nodes **D** and **H** are equal since

$$W_D = W(0)\exp\left[\sigma\left(\sqrt{1-\rho^2}\cdot\left(\Omega_1+2k\sqrt{\Delta t}\right)+\rho\cdot f_y\left(R(2,1)\right)\right)\right] = C(T_1)\exp\left(\sigma\sqrt{1-\rho^2}2k\sqrt{\Delta t}\right)$$
$$= W(0)\exp\left[\sigma\left(\sqrt{1-\rho^2}\cdot\left(\Omega_2+2k\sqrt{\Delta t}\right)+\rho\cdot f_y\left(R(2,2)\right)\right)\right] = W_H,$$

and $G = \frac{\max(C(T_1),W_D)}{\lambda T_2} = \frac{\max(C(T_1),W_H)}{\lambda T_2}$. So we can construct a withdrawal-period tree emitting from these two nodes as illustrated in Fig. 5. Similarly, we can construct another withdrawal-period tree emitting from nodes **F**, **I**, **J**, and **K** in Fig. 4. This is because the guaranteed withdrawal amount G for this tree is $C(T_1)/\lambda T_2$, which can be obtained by substituting the inequality $C(T_1) = W_F = W_I = W_J > W_K$ into Eq. (4).

The structure of the withdrawal-period tree illustrated in Fig. 5 is very similar to that of the deferral-period tree except for the positions of the kinks of the policy value function and the downward jumps of the account value (denoted by the downward arrows) due to the guaranteed withdrawal. Recall that the policyholder can withdraw the guaranteed amount G from the account on the withdrawal dates (time $(T_1+T_2)/2$ and (T_1+T_2) in our example), even if the account value is insufficient to finance the withdrawal. Thus the kinks in the policy value function occur when the account value equals G on the withdrawal dates. To alleviate the oscillation problem described in Fig. 3(a), we should have some tree nodes, say, **c** and **h** in our example, coincide with the kinks. Valid outgoing trinomial branches emitted from the nodes at times T_1 and $(T_1+T_2)/2$ to the following time step can be constructed by the aforementioned mean-tracking method.

The drops in the account value are reflected by the drops in the x coordinates of the nodes on the withdrawal dates. Take node **a** for example. The withdrawal reduces the account value from W_a (denoted by node **a**) to $W_a - G$ (denoted by node **a**′) and the outgoing branches to the next time step are emitted from node **a**′. Similarly, the withdrawal will also change the position of node **b** to **b**′. Note that this downward jump structure will not occur at node **c** and the nodes below **c** (which are not plotted in the figure). This is because withdrawing from the account with insufficient funds will reduce the account value to zero and no more investment will take place. Thus the outgoing branches for the nodes below **c** (inclusive) are not required. Note also that the downward jump structure will not occur at the maturity date. This is because the remaining account value will be returned to policyholders and no more investment will be conducted.

The branch construction method for the withdrawal-period tree is the same as that for the deferral-period tree and is briefly sketched as follows. The converted interest rate tree (colored in gray on the Y–t surface) emits from $f_y(R(2,1))$ and $f_y(R(2,2))$—the projections of node **D** and node **H** on the Y–t surface. This tree can map to part of the Hull–White interest rate tree discussed in panel (a) of Fig. 1. Our withdrawal tree is constructed based on this partial converted interest rate tree. Two trinomial structures, one from node **D** to the nodes at the pillar of $R(3,1)$ and the other from node **a**′ to the nodes at the pillar of $R(4,2)$ are plotted. Other branches are ignored for simplicity. These trinomial structures are also constructed by the mean tracking method. For example, the outgoing trinomial branches from node **D** connect to node **b** and its two adjacent nodes **a** and **c** given that the x coordinate for node **b** $f_x(W_b, R(3,1))$ is closest to the conditional mean $\left(\Omega_1+2k\sqrt{\Delta t}\right)+m_x(T_1,R(2,1))$ among the nodes at the same pillar, where $\Omega_1+2k\sqrt{\Delta t}$ is the x coordinate of node **D**. The outgoing trinomial branch probabilities from node **D** can be obtained by substituting the x coordinates of nodes **a**, **b**, and **c** minus $\Omega_1+2k\sqrt{\Delta t}+m_x(T_1,R(2,1))$ for δ, β, and γ into Eq. (6). Due to the independence of $X(t)$ and $Y(t)$, the branch probabilities from node **D** to nodes **a**, **b**, and **c** are $P''_u p_u$, $P''_u p_m$, and $P''_u p_d$, respectively, where P''_u denotes the branch probability moving from $f_y(R(2,1))$ to $f_y(R(3,1))$. Similarly, the outgoing trinomial branches emitted from other nodes, say, **a**′ and **b**′, can be constructed in a similar way.

3.3. Incorporating a stochastic mortality model into our 3D Tree

Under the assumption that the mortality risk is independent of the investment and the interest rate risks, we can show that a stochastic mortality model can be easily incorporated into our 3D tree without adding an extra dimension to model the evolution of the mortality rate. Let $v\ddot{a}_x(0)$ denote a variable life annuity that is initiated at time 0, with the issue age being x. This annuity is assumed to pay a cash flow U_{t_i} at time t_i, where $i = 1, 2, \ldots, n$, given that the policyholder survives at time t_i. The present value of this annuity can be expressed as the expected value of the lump sum of future discounted cash flows as follows:

$$v\ddot{a}_x(0) = E\left(\sum_{i=1}^{n} U_{t_i}\exp\left(-\int_0^{t_i} r(t)dt\right)\exp\left(-\int_0^{t_i}\mu_t^x dt\right)\right)$$
$$= \sum_{i=1}^{n} E\left(U_{t_i}\exp\left(-\int_0^{t_i} r(t)dt\right)\right) \times E\left(\exp\left(-\int_0^{t_i}\mu_t^x dt\right)\right),$$

where $r(t)$ denotes the short rate defined in Eq. (5), $\exp\left(-\int_0^{t_i} r(t)\,dt\right)$ denotes the present value of one dollar paid at time t_i, μ_t^x denotes the mortality rate defined in Eq. (7), $\exp\left(-\int_0^{t_i}\mu_t^x dt\right)$ denotes the survival rate of the policyholder at time t_i. Obviously, the last equation means that the annuity's value can be expressed as the lump sum of the expected discounted cash flows (without the mortality risk) at each payment date t_i multiplied by the expected survival probability at time t_i. This implies that the mortality risk can be incorporated into our 3D tree by inserting the mortality event into each node with the probability being set to the expected mortality probability evaluated by Eq. (8).

Now we demonstrate how we insert a default event to a node, say, **A** in Fig. 4, as illustrated in Fig. 6. The probability of a policyholder dying within the time interval $[0, \Delta t]$ can be evaluated as $1 - {}_{\Delta t}p_x$ by Eq. (8). Since the mortality risk is independent of the investment and the interest rate risk, each branch probability is changed to the direct multiplication of the original branch probability evaluated in Fig. 4 by the expected survival probability. For example, the branch probability for moving to node **B** is $P_u {}_{\Delta t}p_x$, where P_u and p denote the probability for the process $Y(t)$ moving from $f_y(R(0,1))$ to $f_y(R(1,1))$ and the upward branch probability for the CRR tree, respectively.

3.4. Evaluating a GMWB by the backward induction procedure

A GMWB can be priced by taking advantage of the derivative pricing method as found in many GMXB pricing papers. Specifically, the GMWB value is evaluated as the expected present value of

design, we can imitate the Hull and White (1993) lookback option pricing method by adding extra states to each node of the deferral period tree to remember the maximum account value ever reached. Thus each withdrawal-period tree begins from the states (instead of nodes) of the deferral-period tree that determines the same guaranteed withdrawal amount G.

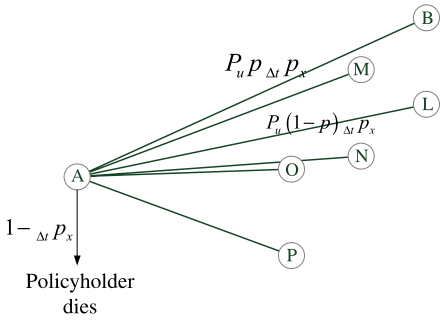

Fig. 6. Inserting a mortality event at node **A**. Notes: The downward arrow denotes a mortality event with a mortality probability listed next to the arrow. The probabilities to move from node **A** to node **B** and from node **A** to node **L** are marked directly on the branches connected to **B** and **L**.

the lump sum of future payments. The backward induction procedure stepwise calculates the expected discounted value from maturity $T_1 + T_2$ back to time 0. For convenience, let V_X denote the GMWB value at the tree node **X**. A policyholder is entitled to withdraw a contractually specified amount G on predetermined withdrawal dates, even when the account value does not meet G. In addition, at the maturity date, the policyholder can receive the remaining funds (if any) from the account after the final withdrawal. Therefore, the GMWB value for an arbitrary node **X** at maturity is $\max(G, W_X)$. Thus, in Fig. 5, the GMWB values for nodes **g**, **h**, and **i** are W_g, $W_h(=G)$, and G, respectively. Each node in our tree either has six outgoing branches (like node **A** in Fig. 4) or nine outgoing branches (like nodes **D** and **a**′ in Fig. 5) plus a mortality branch as in Fig. 6. Assume that the successor nodes connected by a node **z** located at time τ are numbered by $1, 2, \ldots, n$. P_i and V_i denote the probability of reaching the ith node from node **z** and the GMWB value at the ith node, respectively. Then the GMWB value at node **z** can be expressed as the expected discounted GMWB values of the nodes connected by the outgoing branches of node **z** as follows:

$$V_z = e^{-r(z)\Delta t} \sum_{i=1}^{n} P_i V_i + {}_{\Delta t}q_{x+\tau} W_Z, \tag{13}$$

where $r(z)$ denotes the short rate at node **z**, and n denotes the number of outgoing branches from node **z**. The last term in Eq. (13) reflects the provision that the account value is returned to the beneficiary when the policyholder dies. Take node **A** illustrated in Fig. 6 as an example. The GMWB value for node **A** is

$$V_A = e^{-R(0,1)\Delta t} (P_B V_B + P_L V_L + P_M V_M + P_N V_N + P_O V_O + P_P V_P) + {}_{\Delta t}q_x W_A.$$

Note that the short rate $r(A)$ is equal to $R(0, 1)$ since node **A** is located at the pillar of $R(0, 1)$.

At the withdrawal dates, the policyholder can choose either to withdraw the guaranteed withdrawal amount G from the account or to surrender the policy early at the expense of the early redemption penalty. Take node **a** in Fig. 5 as an example. If the policyholder decides to keep the policy, the continuation value (for holding the policy) is the sum of the withdrawal G plus the expected present value of the future income from holding the policy. This expected present value is also the GMWB value for node **a**′ and can be evaluated by Eq. (13). Thus, the continuation value can be expressed as $V_{a'} + G$. On the other hand, the policyholder may decide to surrender the GMWB to receive $G + (1 - k)(W_a - G)$, where k denotes the early redemption penalty. Since the policyholder will decide whether to surrender the policy to maximize the benefit, the GMWB value at node **a** can be expressed as: $V_a = \max(V_{a'} + G, G + (1 - k)(W_a - G))$. The

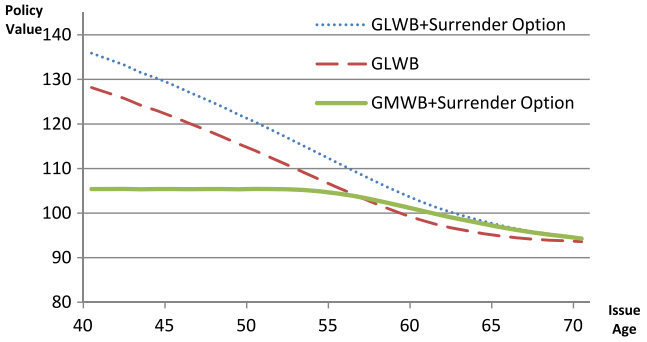

Fig. 7. Comparing the values between GMWBs and GLWBs.[11]

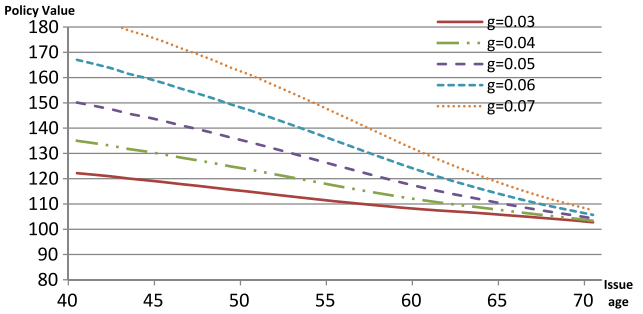

Fig. 8. Comparing the values among GLWBs under different withdrawal ratios.

GMWB values for other nodes at withdrawal dates, say, b, can be evaluated in the same way.

After developing a pricing method for GMWBs, we can iteratively fine tune the insurance fee to find the fair charge α to make the policy a breakeven one; that is, to make the GMWB value equal to the present value of the policyholder's investment. Since the pricing results of our tree converge smoothly as shown by the solid black curve in Fig. 3(a), α can be found by common numerical root finding algorithms such as the bisection method (see Lyuu, 2002).

4. Numerical results

In this section, we first show that our 3D tree model can stably evaluate GMWBs/GLWBs in Section 4.1, and then the comprehensive sensitivity analysis for the fair charges is given in Section 4.2. In the former section, we first show that our tree can generate converging GMWB pricing results without oscillations in Table 2. Then we analyze how the issue age and the withdrawal rate influence GMWB/GLWB values in Figs. 7 and 8, respectively. The comparison of the GMWB and GLWB values is studied. In the latter section, we attempt to study the effect of interest rate risk and mortality risk on the fair charges and surrender options, which cannot be achieved in the existing literature. Our results show that ignoring the interest rate risk will significantly misprice fair charges and surrender option premiums as illustrated in Table 3.On the other hand, ignoring the mortality risk can overestimate these two values as shown in Table 4. Thus we perform all following sensitivity analysis by simultaneously considering the interest rate and the mortality risks. The effects of various factors, such as various provisions (Tables 5, 8, and 11), the length of deferred period (Table 5), the volatility of the account value (from Table 3 to Table 10), the interest rate parameters (Tables 6 and 7),

[11] The policyholder is assumed to invest 100 initially, the insurance fee is set to 0, and the length of the withdrawal period is 10 years. The policyholder can withdraw 2% of the account value per year at the inception of the withdrawal period.

Table 1
Parameter values.

Model	Notation	Definition	Parameter values
Interest rate dynamics	η	Volatility	0.01
	a	Mean reverting rate	0.1
	$r(0)$	Initial short rate	0.0325
Account dynamics	w_0	Initial investments[a]	100
Correlation	ρ	Correlation between $r(t)$ and $W(t)$	−0.25
Mortality	a_D	Mean reverting speed of the stochastic part of the mortality rate Y_t^D	0.5
	b_D	Average level of Y_t^D	−0.035
	σ_D	Volatility of Y_t^D	0.01
GMWB policy	k	Early redemption penalty	0.1
	λ	Number of withdrawal dates per year	1

[a] Under a single premium provision, an investor invests w_0 at time 0. Under a regular premium provision, the lump sum of the present values of all investments equals w_0.

Table 2
Evaluating GMWB values under different scenarios.

	Time steps	$G = 4$ or $g = 4\%$			$G = 5$ or $g = 5\%$			$G = 10$ or $g = 10\%$		
		$(T_1, T_2) = (0, 25)$			$(T_1, T_2) = (0, 20)$			$(T_1, T_2) = (0, 10)$		
		$\sigma = 0.2$	$\sigma = 0.3$	$\sigma = 0.4$	$\sigma = 0.2$	$\sigma = 0.3$	$\sigma = 0.4$	$\sigma = 0.2$	$\sigma = 0.3$	$\sigma = 0.4$
Without mortality risk	100	105.864	112.619	119.361	106.339	113.097	119.803	107.056	113.236	119.341
	200	105.858	112.628	119.438	106.331	113.124	119.924	107.048	113.252	119.432
	1000	105.844	112.630	119.494	106.319	113.124	119.971	107.044	113.252	119.454
	2000	105.841	112.632	119.499	106.317	113.124	119.975	107.043	113.252	119.456
With mortality risk	100	103.887	108.951	114.301	104.985	110.644	116.428	106.600	112.449	118.265
	200	103.881	108.958	114.366	104.977	110.669	116.541	106.591	112.465	118.353
	1000	103.869	108.961	114.414	104.966	110.669	116.584	106.587	112.464	118.375
	2000	103.867	108.960	114.418	104.964	110.667	116.587	106.587	112.464	118.377

Notes: The numbers in the second column denote the time steps in our tree model. The numerical settings used to generate the pricing results follow the settings in Table 1 (if applicable) except the length of the withdrawal period T_2 listed in the first row and the account value volatility σ listed in the second row[a]. The insurance fee is set to zero for examining the accuracy of the tree model under different scenarios.

[a] All the settings for the interest rate model and the policy in the following experiments will also follow the settings in Table 1 unless stated otherwise for consistency.

Table 3
The impacts for introducing the stochastic interest rate on fair charges (unit: bps).

$G = 5$ and $(T_1, T_2) = (0, 20)$ for all cases	Fixed interest rate			Stochastic interest rate $\rho = -0.25$			Stochastic interest rate $\rho = 0.25$		
	$\sigma = 0.2$	$\sigma = 0.3$	$\sigma = 0.4$	$\sigma = 0.2$	$\sigma = 0.3$	$\sigma = 0.4$	$\sigma = 0.2$	$\sigma = 0.3$	$\sigma = 0.4$
No surrender option	66	142	216	62	135	209	78	153	225
with surrender option	66	224	523	62	203	488	79	264	572
Surrender option premium	0	82	307	0	68	279	1	111	347

Notes: The risk-free rate is assumed to be 3.25% under the fixed interest rate assumption. The values of fair charges under this assumption are from Yang and Dai (2013). The stochastic interest rate scenarios follow the settings in Table 1 except the correlations specified in the first row. The mortality risk is not considered in this experiment.

Table 4
Fair charges for GMWBs for deferred life annuities under the stochastic interest rate environment (unit: bps).

Condition		$(T_1, T_2) = (5, 20)$			$(T_1, T_2) = (5, 10)$		
		$\sigma = 0.2$	$\sigma = 0.3$	$\sigma = 0.4$	$\sigma = 0.2$	$\sigma = 0.3$	$\sigma = 0.4$
With mortality risk	No surrender option	111	225	348	218	433	658
	With surrender option	114	325	591	222	523	875
Without mortality risk	No surrender option	125	258	399	233	465	709
	With surrender option	150	429	759	243	582	977

Note: $\rho = -0.25$ in this table.

Table 5
Impacts of roll-up guaranteed and ratchet guaranteed designs.

Condition	$(T_1, T_2) = (5, 10)$			$(T_1, T_2) = (3, 10)$			$(T_1, T_2) = (5, 10)$		
	Roll-up with rate = 3%			Ratchet guarantee			Ratchet guarantee		
	$\sigma = 0.2$	$\sigma = 0.3$	$\sigma = 0.4$	$\sigma = 0.2$	$\sigma = 0.3$	$\sigma = 0.4$	$\sigma = 0.2$	$\sigma = 0.3$	$\sigma = 0.4$
No surrender option	372	647	925	468	934	1498	450	887	1398
With surrender option	445	892	1374	604	1343	2193	541	1171	1897

Notes: The mortality risk is considered in this table and the following experiments.

the correlation between the interest rate and the account value (Tables 3 and 7), the mortality risk parameters (Tables 9 and 10), and their joint effects on fair charge and surrender option premiums of GMWBs/GLWBs are discussed.

For simplicity, we first assume that a policyholder invests a single premium with a deferred variable annuity associated with a GMWB policy. The settings for the interest rate model and the GMWB policy in the following experiments are shown in Table 1

Table 6
Impacts of the long-term interest rate level ($\theta(t)$) on the fair charges for GMWBs $(T_1, T_2) = (0, 20)$ (unit: bps).

Condition	$\theta(t) = 1.5\%$			$\theta(t) = 3.25\%$			$\theta(t) = 5\%$		
	$\sigma = 0.2$	$\sigma = 0.3$	$\sigma = 0.4$	$\sigma = 0.2$	$\sigma = 0.3$	$\sigma = 0.4$	$\sigma = 0.2$	$\sigma = 0.3$	$\sigma = 0.4$
No surrender option	125	225	319	51	114	179	21	62	108
With surrender option	136	389	750	51	131	326	21	62	132

Table 7
Impacts of interest rate volatility (η) and the correlation (ρ) on the fair charges for GMWBs $(T_1, T_2) = (0, 10)$ (unit: bps).

Condition	$\rho = -0.8$		$\rho = 0$		$\rho = 0.8$	
	$\eta = 0.01$	$\eta = 0.02$	$\eta = 0.01$	$\eta = 0.02$	$\eta = 0.01$	$\eta = 0.02$
No surrender option	128	100	166	176	200	241
With surrender option	128	100	166	177	205	273

Table 8
Comparing the fair charges and the surrender option premiums for GMWBs and GLWBs (unit: bps).

Conditions		$\sigma = 0.2$	$\sigma = 0.3$	$\sigma = 0.4$
GLWB	With surrender option	75	168	303
	Without surrender option	75	158	245
GMWB	With surrender option	52	109	212
	Without surrender option	52	107	165

Notes: $(T_1, T_2) = (0, 20)$ in a GMWB policy. The guaranteed withdrawal ratio g is set to 5%.

unless stated otherwise. To provide a fair comparison between the fixed and the stochastic interest rate environments, the fixed interest rate and the function of the long-term interest rate $\theta(t)$ (defined in Eq. (5)) are assumed to be a constant 3.25% unless stated otherwise. For convenience, we use the pair (T_1, T_2) to indicate that the lengths of the deferral period and the withdrawal period are T_1 and T_2, respectively.

4.1. Evaluating the GMWBs/GLWBs

Evaluating a GMWB/GLWB policy with a naïve tree might result in oscillating pricing results as plotted by the thin gray curve in Fig. 3(a), and this unwelcome property will prevent us from accurately finding the fair charge α. To alleviate the oscillation problem, our tree is adjusted to coincide with the critical locations. Thus the pricing results generated by our tree model illustrated in Table 2 converge smoothly and quickly with the increment in the number of time steps of the tree n (listed in the second column). Even incorporating the stochastic mortality rates will not lead to deterioration in this smoothing convergence property. Indeed, this property will generate smoothing pricing results as illustrated by the solid black curve in Fig. 3(a) and will help us to accurately find fair charges.

A simple sensitivity analysis for the GMWB values in Table 2 is provided as follows. Here we focus on immediate life annuities (i.e., $T_1 = 0$) and the deferred annuities (i.e., $T_1 \neq 0$) will be discussed later. We first compare how the lengths of the guaranteed withdrawal periods T_2 listed in the first row influence the values of the GMWBs. Increasing T_2 (or decreasing the guaranteed withdrawal amount G) implies that some withdrawal payments are postponed and the policyholder loses the time value of the withdrawals. Therefore, a GMWB value decreases with the increment of T_2 to reflect the loss of time value. Besides, it can be observed that the value of a GMWB increases with the volatility of the account value σ. This is because a GMWB can be roughly decomposed into an annuity plus a call option on the remaining account value (after periodical withdrawals during the withdrawal period) at maturity and that the call option value increases with σ. Finally, incorporating the mortality risk would reduce the GMWB value, since the withdrawal guarantee will be annulled due to the death of the policyholder.

Now we compare the difference between a GMWB policy with a limited withdrawal period and a GLWB policy with a lifelong withdrawal period in Fig. 7. The withdrawal amount is set as 2% of the account value at the inception of the withdrawal period. The issue age of the policyholder has very little impact on the GMWB value when the issue age is not too high. This is because most young policyholders could survive to the end of the withdrawal period. However, when the issue age is high, the increasing mortality risk is more likely to annul the withdrawal guarantee and to reduce the GMWB value. On the other hand, a GLWB policy provides a lifelong withdrawal guarantee. This implies that the total amounts that can be withdrawn from a GLWB are highly related to the life expectancy of the policyholder. That is why the GLWB value decreases with the increment of the issue age. Note that a GLWB value would converge to the GMWB value when the issue age is high, say, 70 in this example. This is because a higher issue age is

Table 9
The impacts of changing the mortality parameters a_D, b_D, and σ_D on the fair charges (unit: bps).

	$b_D = -0.035$			$a_D = 0.5$		
	$a_D = 0.4$	$a_D = 0.5$	$a_D = 0.6$	$b_D = -0.035$	$b_D = -0.025$	$b_D = -0.015$
$\sigma_D = 0.01$	347.58	350.19	351.84	350.19	327.36	306.24
$\sigma_D = 0.02$	349.58	351.45	352.88	351.45	328.60	307.40
$\sigma_D = 0.03$	352.88	353.76	354.64	353.76	330.91	309.16

Table 10
The impacts of changing the mortality parameters a_D and b_D and the account value volatility σ on the fair charges (unit: bps).

	$b_D = -0.035$			$a_D = 0.5$		
	$a_D = 0.4$	$a_D = 0.5$	$a_D = 0.6$	$b_D = -0.035$	$b_D = -0.025$	$b_D = -0.015$
$\sigma = 0.2$	152.57	153.53	154.08	153.53	145.29	137.55
$\sigma = 0.3$	347.58	350.19	351.84	350.19	327.36	306.24
$\sigma = 0.4$	577.06	582.00	585.30	582.00	538.74	499.26

more likely to result in the policyholder having a higher chance of dying prior to the end of the withdrawal period, and making the cash flow pattern of a GMWB more similar to that of a GLWB. Next, we focus on the impact of the presence of the surrender option on the GLWB value. The difference between the dotted line (the GLWB with a surrender option) and the dashed line (the GLWB without a surrender option) can be viewed as the premium of the surrender option. This value decreases with the increment of the issue age. This is because a higher issue age implies a higher mortality risk that makes the policy more likely to be terminated early due to the death of the policyholder. This early termination reduces the option value.

Fig. 8 suggests that the GLWB value increases with the increment of the guaranteed withdrawal ratio g. This incremental property is more significant than the property of the GMWB value increment observed in Table 2. This is because, in a GMWB policy, the increment of g entails a decrement in the length of the withdrawal period T_2 as described in Eq. (4). On the other hand, a GLWB policy provides a lifelong withdrawal guarantee which is not influenced by g. Besides, the value increment due to the increment of g will decrease as the issue age increases. This is because a higher issue age implies a higher mortality risk that is more likely to annul the guaranteed withdrawals.

4.2. Sensitivity analyses for fair charges

Comparisons between fixed/stochastic interest rate assumptions

The insurance company receives the fee withdrawn from the account during the lifetime of the policy in return for the investment guarantee and other policy provisions. Evaluating the break even insurance fee, or the fair charge α, is thus important for issuing GMWBs/GLWBs. Yang and Dai (2013) analyze the impacts of different GMWB provisions on fair charges without considering the impacts of the randomness of the interest rate. The numerical results in Table 3 compare fair charges under the constant and the stochastic interest rate assumptions and show that ignoring the randomness of the interest rate will overprice (underprice) fair charges given the correlation between the interest rate and the account value ρ is large (small). For example, given that $\rho = 0.25$ and the volatility of the account $\sigma = 0.3$, introducing the randomness of the interest rate would increase the fair charge from 142 basis points (bps) to 153 bps if the surrender option provision were absent (or from 224 bps to 264 bps if the surrender option were present). On the other hand, a smaller ρ, -0.25, would reduce the fair charge from 142 basis points (bps) to 135 bps if the surrender option provision were absent (or from 224 bps to 203 bps if the surrender option were present).

Yang and Dai (2013) also suggest that introducing the surrender option will increase fair charges, and their findings are confirmed in Table 3. In addition, incorporating the randomness of the interest rate would further enhance (reduce) the impact given the correlation ρ is large (small). Recall that the surrender option grants the policyholder the right to redeem the policy early at the cost of a higher fair charge—call it the surrender option premium for simplicity. Under the fixed interest rate assumption, the presence of the surrender option would increase the fair charge from 142 bps to 224 bps given that the volatility of the account $\sigma = 0.3$; the surrender option premium is 82 bps (=224–142). On the other hand, under the stochastic interest rate assumption, the surrender option premium would either increase to 111 bps (=264–153) given $\rho = 0.25$ or decrease to 68 bps given $\rho = -0.25$.

It can be observed that the increment (or decrement) of the account value volatility σ would also increase (or decrease) the hedge cost and as a consequence the fair charge and the surrender option premium. For example, under the fixed interest rate assumption, increasing the volatility σ from 0.3 to 0.4 would increase the fair charge from 142 bps to 216 bps given that the surrender option is absent (or from 224 bps to 523 bps given that the surrender option is present). The surrender option premium would further increase from 82 bps to 307 bps. On the other hand, decreasing the volatility σ from 0.3 to 0.2 would decrease the fair charge to less than 100 bps and make the surrender option valueless. Introducing the randomness of the interest rate could further enhance (reduce) the impacts of changing σ on the surrender option premium given ρ is large (small). Compared to the premium increment 225 bps (=307–82) due to the increment of σ from 0.3 to 0.4 under the fixed interest rate assumption, the increment would further rise (fall) to 236 bps (211 bps) given that $\rho = 0.25$ ($\rho = -0.25$). The aforementioned changes in fair charges and option premiums reflect the cost faced by the insurance company in hedging the interest rate risk. When ρ is small, a considerable part of the interest rate risk and the account value risk are neutralized. Thus, introducing the interest rate risk would decrease both fair charges and option premiums. On the other hand, this neutralization effect becomes insignificant with a larger ρ and introducing the interest rate risk will increase fair charges and option premiums. This finding is consistent to the finding of Peng et al. (2012). The above phenomena imply that ignoring the interest rate risk might significantly misprice GMWBs. Thus, the stochastic interest rate settings will be taken into account in the following experiments unless stated otherwise.[12]

The following experiments focus on five issues in GMWBs/GLWBs: First, we reexamine the impacts of various GMWB provisions in Yang and Dai (2013) on fair charges under the stochastic interest rate assumption. Second, we analyze how different parameters of the stochastic interest rate model influence the fair charges of GMWBs. Third, we compare fair charges between the GMWB and GLWB policies. Since a GLWB provides a lifelong withdrawal guarantee, the mortality risk plays an important role in pricing a GLWB policy. The fourth topic analyzes how the parameters of the mortality model influence the fair charges of GLWBs. Finally, Yang and Dai (2013) argue that their numerical evaluation model can faithfully model the jumps of the account value due to discrete withdrawals. They claim that the discrete withdrawal setting is more typical than the continuous withdrawal one which is widely adopted in the previous literature. Our experiments suggest that the withdrawal settings do not influence the fair charge much. On the other hand, the feature to model the jumps of the account value can be used to evaluate the policy with a regular premium provision. The regular premium setting is more popular than the single premium setting. However, many studies only analyze the latter setting. Our experiments show how regular premium settings significantly influence fair charges.

Analyzing the impacts of policy provisions on fair charges

We analyze the impacts of deferred guaranteed withdrawals and corresponding provisions under the stochastic interest rate assumption in this subsection. Note that the above numerical analyses rely on the immediate guarantee withdrawal assumption; that is, the deferral period is absent (or $T_1 = 0$). Although many studies

[12] Yang and Dai (2013) program spend less computational time than our program but their program ignores the interest rate risk. We run both programs on a Win2003 computer with an Intel Core2 Duo CPU @2.53 GHz and 2 GB RAM. It cost about 132 s and 12 s to run our program and Yang and Dai's program on a 100-time-step tree, respectively. Although our program spends 120 s more than Yang and Dai's program to model the interest rate risk, the experimental results in Table 3 suggests that ignoring the interest rate risk might significantly misprice fair charges and surrender option premiums.

adopt this assumption to keep their analyses simple, most GMWB policies are deferred variable annuities. In addition, ignoring the impact of deferring withdrawals significantly misprices the fair charge, which can be observed by comparing Tables 3 and 4. A 5-year deferral period is inserted into each case of Table 4 and the lump sum of the guaranteed withdrawal amount is protected by the principal guarantee; that is, $C(T_1)$ in Eq. (4) is set to the present value of investment w_0. Thus, we can compare the "$\rho = -0.25$ column" in Table 3 with the "$(T_1, T_2) = (5, 20)$" column in Table 4.[13] Here we first focus on the case that does not incorporate the mortality risk to make our analysis focus on the presence of the deferral period. It can be observed that the insertion of the deferral period will further increase the fair charge from 135 bps (see Table 3) to 258 bps (see Table 4) given that $\sigma = 0.3$ and that the surrender option is absent. This is because the principal guarantee provides the downside protection on the policyholder's investment. This benefit is more than the loss of the time value due to the postponement of the guaranteed withdrawals caused by the insertion of the deferral period.

Ignoring the mortality risk will overprice the fair charge and the surrender option premium as illustrated in Table 4. This is because both the guaranteed withdrawal and the surrender option provision will be annulled due to the death of the policyholder. For example, given $\sigma = 0.3$, incorporating the mortality risk reduces the fair charge from 258 bps to 225 bps given that the surrender option is absent (or from 429 bps to 325 bps given that the surrender option is present). The surrender option premium declines from 171 bps (=429–258) to 100 bps (=325–225). To avoid the bias, the mortality risk will be taken into account in the following experiments unless stated otherwise.

Besides, Table 4 also compares how the length of the withdrawal period influences fair charges. Recall that reducing the length of the withdrawal period T_2 from 20 years to 10 years would increase the guaranteed withdrawal amount G as defined in Eq. (4). This implies that the policyholder can receive the guaranteed payments earlier and reduce the loss of time value. Thus the insurance company should receive a higher insurance fee in return for offering early guarantee payments. For example, reducing T_2 from 20 years to 10 years would increase the fair charge from 399 bps to 709 bps given that $\sigma = 0.4$ and that both the mortality risk and the surrender option are absent.

Besides, the effects of changing the account value volatility σ on the fair charge for a deferred variable annuity in Table 4 are similar to those for an immediate variable annuity illustrated in Table 3. Thus we ignore the detailed analyses for simplicity.

The roll-up interest rate and ratchet guarantee designs are both popular in variable deferred annuities, and the significant increment in the fair charge due to these two guarantee designs can be observed by comparing Table 4 with Table 5. A i% roll-up interest rate guarantee ensures that the policyholder will receive $w_0(1 + T_1)^i$ instead of w_0 determined in the principal guarantee. Granting extra 3% return would increase the fair charge from 222 bps (see Table 4) to 445 bps (see Table 5) given that $\sigma = 0.2$, $(T_1, T_2) = (5, 10)$, and the surrender option provision is present. Replacing the rollup interest guarantee design by the ratchet guarantee design without changing other settings would further increase the fair charge to 541 bps. It is obvious that ignoring the impacts of the guarantee designs would significantly misprice the fair charge.

Numerical experiments for analyzing the ratchet guarantee design under different deferral period are also illustrated in Table 5. Based on the same guaranteed withdrawal period of 10 years, we find that both the fair charge and the surrender option premium decrease with the increment of the deferral period. This is because increasing the deferral period implies that the policyholder would lose the time value due to the postponed withdrawal. Even though a longer deferral period may provide a higher guaranteed withdrawal based on the mechanism of the ratchet guaranteed design, the loss of time value due to the postponed withdrawal cannot be compensated by the gain from the possible increment of guaranteed withdrawals. According to the above analyses, we conclude that a valuation method capable of pricing different guaranteed designs is essential for pricing fair charges.

Sensitivity analyses of the interest rate model parameters

Now we examine how the changes in interest rate parameters, like the long term interest rate level $\theta(t)$, the correlation between the short rate and the account value ρ, and the short rate volatility η of the Hull and White (1990) model, influence the fair charges in Table 6. We set the long-term interest rate level $\theta(t)$ as a constant function of time t. The numerical results suggest that both the fair charge and the surrender option premium decrease with the increment of $\theta(t)$. For example, under the condition of $\sigma = 0.3$, increasing $\theta(t)$ from 1.5% to 3.25% decreases the fair charge from 225 bps to 114 bps given that the surrender option is absent (or from 389 bps to 131 bps given that the surrender option is present). This is because increasing $\theta(t)$ will decrease the insurance company's obligation, i.e. the present values of future guaranteed withdrawals. Besides, the surrender option premium also dramatically decreases from 164 bps (=389–225) to 17 bps (131–114). Note also that increasing $\theta(t)$ further to 5% would even make the surrender option valueless.

The impacts of different interest rate volatilities η and the correlations between the interest rate and the account value on the fair charges ρ are studied in Table 7. When the correlation ρ is large (small), the fair charge increases (decreases) with the increment of the interest rate volatility. For example, given that the surrender option is absent, increasing η from 0.01 to 0.02 will increase the fair charge from 200 bps to 241 bps if ρ is 0.8 (but decrease the fair charge from 128 bps to 100 bps if $\rho = -0.8$). Similarly, the impacts of increasing the interest rate volatility η on the surrender option premium also increase as the correlation ρ increases. For example, when $\sigma = 0$, increasing η from 0.01 to 0.02 increases the surrender option premium from 0 bps (=166–166) to 1 bps (=177–176). However, when ρ increases to 0.8, increasing η will dramatically increase the surrender option premium from 5 bps (=205–200) to 32 bps (=273–241). Thus, ignoring the impacts of the stochastic interest rate will significantly misprice the fair charge and the surrender option premium.

Comparison between GMWBs and GLWBs

Now we compare GMWB and GLWB policies as illustrated in Table 8. In contrast to a GMWB policy that offers a limited withdrawal period, say $T_2 = 20$ years, a GLWB policy offers a lifelong withdrawal guarantee. Here the guaranteed withdrawal ratio for both GMWB and GLWB are set to 5% so we can focus our analyses on the impact between the limited and the lifelong withdrawal guarantees. Obviously, a GLWB issuer receives a higher fair charge than a GMWB issuer in return for offering a longer withdrawal guarantee. A longer guarantee also increases the likelihood of the policyholder exercising the surrender option. Thus, the surrender option premium for a GLWB policy is higher than a GMWB one given all other conditions being equal. Besides, it can be observed that both the fair charge and the surrender option premium of a GLWB increase with the increment of σ, which is analogous to the aforementioned property for a GMWB policy. Indeed, the results of the sensitivity analysis for both the GMWB and GLWB policies are quite similar. Thus, in the following experiments, we will focus on GLWBs for simplicity.

[13] This ensures that the numerical settings for both scenarios are the same except the length of the deferral period T_1, which are 0 and 5 for Tables 3 and 4, respectively.

Table 11
The impacts of changing investment/withdrawal frequencies on fair charges (unit: bps).

Frequency	Single premium	Annual premium	Semiannual premium	Seasonal premium	Monthly premium
Annual withdrawals	350.19	532.70	551.73	563.82	572.53
Semiannual withdrawals	351.12	534.37	553.57	565.58	574.37
Seasonal withdrawals	351.34	535.24	554.48	566.33	575.24
Continuous withdrawals	352.00	535.91	555.25	567.09	575.96

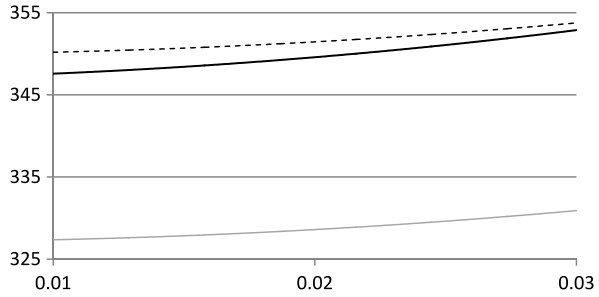

Fig. 9. The impacts of changing σ_D on the fair charges. Notes: The x- and y- axes denote σ_D and fair charge, respectively. The black-solid line, black-dotted line, and the gray line denote the case that $a_D = 0.4$ and $b_D = -0.035$, $a_D = 0.5$ and $b_D = -0.035$, and $a_D = 0.4$ and $b_D = -0.025$.

The mortality risk and the investment risk

The impacts of mortality risk and investment risk on the fair charges are analyzed in Tables 9 and 10.[14] Since the mortality dynamics are governed by the underlying parameters of (a_D, b_D, σ_D) as shown in Eq. (7), we examine different parameter values on the fair charges. It can be observed that the fair charge increases with the increment of the mean reverting speed (a_D) and the volatility (σ_D) of the stochastic part of the mortality rate Y_t^D. To see the effect resulting from mortality risk parameter (σ_D), Fig. 9 presents how the fair charge is sensitive to the increment of the mortality risk parameter σ_D. This is because the more volatile the mortality rate is, the higher the hedge cost of the mortality risk (and as a consequence the fair charge) that will be incurred. On the other hand, b_D can be viewed as the long-term average level of Y_t^D. That is, a lower b_D on average implies a lower mortality rate and a longer life expectancy. It could then result in a longer withdrawal period, and thus a higher fair charge. Similarly, increasing the volatility of the account value $\boldsymbol{\sigma}$ will also increase the hedge cost and the fair charge as illustrated in Table 10. The insurer cannot ignore the trend of mortality improvement and volatility in pricing GMWB/GLWB policies.

The impacts of withdrawal frequencies and single/regular premiums

Discrete investments and withdrawals would lead to jumps in the account value as in Eqs. (1) and (3) and make the evaluation problem intractable. To simplify this problem, many studies adopt continuous withdrawals and the single premium provision, which is uncommon in insurance markets. Yang and Dai (2013) argue that replacing discrete withdrawals with continuous ones may significantly misprice the fair charge, while Dai et al. (2008) argue that different withdrawal frequencies do not influence the fair charge that much. To clarify the conflict, we analyze the impacts of withdrawal frequencies in Table 11. It seems that increasing the withdrawal frequencies only mildly increases the fair charges. This is because a higher withdrawal frequency accelerates the speed of receiving guaranteed withdrawals and reduces the loss of time value. On the other hand, we find that replacing a regular premium provision with a single one or decreasing investment frequencies significantly reduces fair charges. To keep the comparisons fair, the investment amounts for all investment frequencies are appropriately set to make the lump sum of the present values (under different frequencies) equal.

[14] In Tables 9–11, the length of the deferral period T_1 is 10 years and all other parameters follow the settings in Table 1 unless explicitly stated in this table.

5. Conclusion

Granting GMWBs has emerged as a key component associated with variable annuity products in investment and retirement income systems. The life span of a GMWB can be longer than a decade or even be lifelong (i.e., a GLWB). In addition to the investment risk, both the interest rate risk and the mortality risk play significant roles in evaluating such a long-term policy. Evaluating GMWBs/GLWBs has drawn much attention in both academia and in practical fields because such policies are popular and have many complex provisions that need to be dealt with. As a result, analyzing the impacts of the aforementioned risks and provisions in valuing GMWBs/GLWBs has become a critical issue in developing the variable guarantee and has also become a great challenge to the insurer.

To address the aforementioned issue, this paper proposes a 3D tree that can analyze the interaction impacts of the aforementioned risks and provisions on the value and the fair charge of a GMWB/GLWB. The structure of our 3D tree is sophisticatedly designed to avoid the unstable (oscillating) pricing results phenomenon that is a characteristic of many numerical pricing methods. To the best of our knowledge, this paper is the first one to deal with investment, interest rate and mortality rate risk simultaneously without losing the realistic product feature in dealing with the most popular guarantee designs of GMWB/GLWB contracts. Thus, the main contribution of this paper is to build up the valuation framework that can further include a stochastic interest rate model and a stochastic mortality model for GMWB and GLWB contracts, extending Yang and Dai (2013). With such a realistic valuation framework, we can identify some important findings which cannot be observed using the existing model. First, comparing to fixed-interest-rate scenarios evaluated in Yang and Dai (2013) model, introducing the interest rate risk significantly influence fair charges and surrender option premiums. Our tree model can stably price the interest rate risk. In addition, the significant impacts of changing interest rate volatility as well as the correlation between the short rate and the account value on fair charges can be analyzed by our tree model. Second, we can capture the longevity risk to value both GMWB and GLWB contracts. We compare the difference between a GMWB policy with a limited withdrawal period and a GLWB policy with a lifelong withdrawal period. Third, the values of the popular provisions and the surrender option associating with GMWB/GLWB contracts could be affected by not only the future investment uncertainty but also the interest rate and mortality rate risks. The proposed 3-D tree model can analyze the popular provisions and the surrender option under a stochastic investment, interest rate and mortality rate environment simultaneously.

Some effects regarding the interaction among the policy provisions, investment risk, mortality risk, and interest rate risk on the evaluation of GMWBs/GLWBs are important and worth emphasizing here. Our analysis suggests that both the fair charge and the surrender option premium increase with the increment

of the volatility level of the investment account and the mortality rate. They decrease with the increment of the length of the deferral period and the long-term interest rate level. The impact of the interest rate volatility on the fair charge depends on the correlation between the interest rate and the account value. The comparisons between immediate and deferred withdrawals, single and regular premiums, as well as between principal guarantee, rollup interest guarantee and ratchet guarantee designs are also well studied in our paper. Our analysis also shows that evaluating GMWBs/GLWBs without considering the impacts of interest rate risk, mortality risk, and the aforementioned provisions may result in significant pricing errors. These numerical findings are critical in developing, pricing, and hedging GMWB/GLWB contracts.

In this paper, we incorporate the stochastic mortality model proposed by Biffis (2005) and the interest rate model by Hull and White (1994) in our pricing model and show that changing the model's parameters could significantly influence the evaluation of GMWBs/GLWBs. Our analysis suggests that the selection of financial and mortality models and the calibration of model parameters are critical in evaluating GMWBs/GLWBs and deserve to be studied further. Indeed, the insurer may determine a proper mortality model and parameters based on the insurer's mortality experience in order to capture the randomness of mortality rates due to longevity risk and the occasional spread of high-lethal-rate diseases. In addition, the financial models shall be calibrated to the market condition. We believe that insurers can discover an appropriate mortality model for capturing longevity risk and financial models to apply our proposed 3D tree model for pricing GMWBs/GLWBs.

Acknowledgments

We thank Chang, Kuo-Pei and Hsu, Chien-Hsun for programming. The first author was supported in part by the MOST 103-2410-H-009 -003 -MY3. The second author was supported in part by the MOST grant 102-2628-H-008 -001 -MY3. The third author was supported in part by the MOST 103-2410-H-009 -003 -MY3.

References

Bauer, D., Kling, A., Russ, J., 2008. A universal pricing framework for guaranteed minimum benefits in variable annuities. ASTIN Bull. 38, 621–651.
Biffis, E., 2005. Affine processes for dynamic mortality and actuarial valuations. Insurance Math. Econom. 37 (3), 443–468.
Chen, Z., Vetzal, K., Forsyth, P.H., 2008. The efficiency of modelling parameters on the value of GMWB guarantees. Insurance Math. Econom. 43, 165–173.
Costabile, M., Massabó, I., Russo, E., 2008. A binomial model for valuing equity-linked policies embedding surrender options. Insurance Math. Econom. 42, 873–886.
Cox, J.C., Ross, S., Rubinstein, M., 1979. Option pricing: A simplified approach. J. Financ. Econ. 7, 229–264.
Dai, T.-S., 2009. Efficient option pricing on stocks paying discrete or path-dependent dividends with the stair tree. Quant. Finance 9, 827–838.
Dai, M., Kowk, Y.K., Zong, J., 2008. Guaranteed minimum withdrawal benefit in variable annuities. Math. Finance 18, 595–611.
Dai, T.-S., Lyuu, Y.-D., 2010. The bino-trinomial tree: A simple model for efficient and accurate option pricing. J. Deriv. 17, 7–24.
Duffie, D., 1996. Dynamic Asset Pricing Theory, second ed. Princeton University Press, Princeton, NJ.
Figlewski, S., Gao, B., 1999. The adaptive mesh model: A new approach to efficient option pricing. J. Financ. Econ. 53, 313–351.
Fung, M.C., Ignatieva, K., Sherris, M., 2013. Systematic mortality risk: An analysis of guaranteed lifetime withdrawal benefits in variable annuities. In: Colloquium of the International Actuarial Association, Lyon, France.
Holz, D., Kling, A., Russ, J., 2012. GMWB for life: An analysis of lifelong withdrawal guarantees. Z. Gesamte Versicher. 101, 305–325.
Hull, J., White, A., 1990. Pricing interest-rate-derivative securities. Rev. Financ. Stud. 3, 573–592.
Hull, J., White, A., 1993. Efficient procedures for valuing European and American path-dependent options. J. Deriv. 1, 21–31.
Hull, J., White, A., 1994. Numerical procedures for implementing term structure models II. J. Deriv. 2, 37–48.
IASB, 2001. Draft Statement of Principles. International Accounting Standards Board, London.
IASB, 2004. International Financial Reporting Standard No. 4. International Accounting Standards Board, London.
Kijima, M., Wong, T., 2007. Pricing of ratchet equity-indexed annuities under stochastic interest rates. Insurance Math. Econom. 41, 317–338.
LIMRA, 2013. VA GLB Election Tracking Survey.
Lin, X.S., Tan, K.S., 2003. Valuation of equity-indexed annuities under stochastic interest rates. N. Am. Actuar. J. 8, 72–125.
Lyuu, Y.D., 2002. Financial Engineering and Computation: Principles, Mathematics, and Algorithms. Cambridge University Press, Cambridge, UK.
Lyuu, Y.-D., Wang, C.-J., 2011. On the construction and complexity of the bivariate lattice with stochastic interest rate models. Comput. Math. Appl. 61 (4), 1107–1121.
Milevsky, M.A., Salisbury, T.S., 2006. Financial valuation of guaranteed minimum withdrawal benefits. Insurance Math. Econom. 38, 21–38.
Nielsen, J.A., Sandmann, K., 1995. Equity-linked life insurance—A model with stochastic interest rates. Insurance Math. Econom. 16, 225–253.
Otar, J., 2007. Variable annuities primer GMWBs are making inroads into Canada, but how do they stand up to market history? Anal. Perspect. Canada's Financ. Prof. 5 (3), 11.
Peng, J., Leung, K.S., Kwok, Y.K., 2012. Pricing guaranteed minimum withdrawal benefits under stochastic interest rates. Quant. Finance 12 (6), 933–941.
Piscopo, G., Haberman, S., 2011. The valuation of guaranteed lifelong withdrawal benefit options in variable annuity contracts and the impact of mortality risk. N. Am. Actuar. J. 15 (1), 59–76.
Shen, W., Xu, H., 2005. The valuation of unit-linked policies with or without surrender options. Insurance Math. Econom. 36 (1), 79–92.
Vasicek, O.A., 1977. An equilibrium characterization of the term structure. J. Financ. Econ. 5, 177–188.
Yang, S.S., Dai, T.-S., 2013. A flexible tree for evaluating guaranteed minimum withdrawal benefits under deferred life annuity contracts with various provisions. Insurance Math. Econom. 52 (2), 231–242.
Zvan, R., Forsyth, P., Vetzal, K., 2003. Negative coefficients in two-factor option pricing models. J. Comput. Finance 7 (1), 37–74.